Biostimulation of jarosite and iron oxide-bearing mine waste enhances subsequent metal recovery

Mark Roberts[a1], Pallavee Srivastava[a]*, Gordon Webster[b], Andrew J Weightman[b], Devin J Sapsford[a]

[a] School of Engineering, Cardiff University, Queen's Building, The Parade, Cardiff CF24 3AA. United Kingdom; [b] School of Biosciences, Cardiff University, Sir Martin Evans Building, Museum Avenue, Cardiff, CF10 3AX. United Kingdom

* Corresponding Author

Address: School of Engineering, Cardiff University, Queen's Building, The Parade, Cardiff CF24 3AA United Kingdom

Phone: +44 7512059984

e-mail: srivastavap5@cardiff.ac.uk

Abbreviations:

EDTA- Ethylenediaminetetraacetic acid

IMWs- Industrial and mining wastes

PLS- Pickle liquor sludges

DIRM- Dissimilatory iron reducing microorganisms

PSD- Particle size distribution

TC- Total carbon

TOC- Total organic carbon

TIC- Total inorganic carbon

HDPE- High density polyethylene

DIW- Deionised water

ORP-Oxidation-reduction potential

EC- Electrical conductivity

DO- Dissolved oxygen

NGS- Next-generation sequencing

XRD- X-ray diffraction

[1] Presently at Geochemic Ltd, Lower Race, Pontypool, NP4 5UH

AMD- Acid mine drainage

Abstract

Novel resource recovery technologies are required for metals-bearing hazardous wastes in order to achieve circular economy outcomes and industrial symbiosis. Iron oxide and co-occurring hydroxysulphate-bearing wastes are globally abundant and often contain other elements of value. This work addresses the biostimulation of indigenous microbial communities within an iron oxide/ hydroxysulphate-bearing waste and its effect on the subsequent recoverability of metals by hydrochloric, sulphuric, citric acids and EDTA. Laboratory-scale flow-through column reactors were used to examine the effect of using glycerol (10% w/w) to stimulate the *in situ* microbial community in an iron oxide/ hydroxysulphate-bearing mine waste. The effects on the evolution of leachate chemistry, changes in microbiological community and subsequent hydrometallurgical extractability of metals were studied. Results demonstrated increased leachability and selectivity of Pb, Cu, and Zn relative to iron after biostimulation with a total of 0.027 kg of glycerol per kg of waste. Biostimulation, which can be readily applied *in situ*, potentially opens new routes to metal recovery from globally abundant waste streams that contain jarosite and iron oxides.

Environmental Implication

Large quantities of iron oxide/hydroxysulphate bearing wastes are generated every year which present a potential exploitable iron resource along with being suited for recovery of other co-occurring metals. Resource recovery from these 'jarosite-type' material renders them safe for application in various domains. This study exhibits the circular economy route of making metals present within the iron-rich waste more susceptible to acid/chelator leaching post biostimulation in presence of glycerol, a waste by-product of biodiesel manufacturing industry. The indigenous microorganisms present in the waste were responsible of movement of metals from less reactive to more reactive phases.

Introduction

The "technosphere" includes any material established by human agency in contrast to lithospheric stocks established by geological processes (Johansson et al., 2013). Iron oxide minerals include the wide variety of iron oxides, hydrous ferric oxides, hydroxides, oxyhydroxides, and co-occurring hydroxysulphate minerals found within many industrial and mining wastes (IMWs). Billions of tonnes of IMWs have been produced and continued global arisings are in the hundreds of millions of tonnes annually. As the world moves towards circular economies, iron oxide/ hydroxysulphate-bearing wastes (hereon in "iron-rich" waste) present a potentially exploitable technospheric iron resource, as well as a source of other elements of strategic and/or economic value that have been sequestered via sorption, coprecipitation or occlusion with the iron-rich waste (Roberts et al., 2020).

Notable examples of large arisings of iron-rich wastes include Zn refinery residues, red mud (bauxite ore processing residue), pickle liquor sludges from steel making (PLS), mine wastes, and mine water treatment residues. For example, Pelino et al., (1997) reported that 750,000 tonnes of Zn refinery residue were produced in the European Union alone. Zn refinery residues are grouped as "jarosite-type" with higher sulphur content (~10-12%), dominated by jarosite with other metal sulphates and hydroxides, or as "goethite-type" dominated by goethite, maghemite, and magnetite. These residues have been studied for recovery of Zn, Pb, Ag, Cu, Ca, Fe, and In (Han et al., 2014; Ju et al., 2011; C. Liu et al., 2017). An estimated 2.7 billion tonnes of red mud had been accumulated globally by 2007, increasing by 120 Mtpa (Power et al., 2011), by this estimate bringing the current inventory to 4.5 billion tonnes. Red mud can contain elevated concentrations of Al, Cr, Cu, Ga, Ni, Mo, Sc, U, V, and Zn along with Rare Earth Elements (Binnemans et al., 2013; Borra et al., 2015; Y. Liu & Naidu, 2014; Wang et al., 2013). PLS is an iron-rich residue produced during iron and steelmaking from the acidic stripping of oxidised layers from the final steel product. The acidic effluent is neutralised and produces the sludge. Common constituents are Cr_2O_3 (~5-11 wt.%), SiO_2 (~1-9 wt.%), NiO (~1-2 wt.%), Al_2O_3 (~3 wt.%) and ZnO, TiO_2, and CuO/ Cu_2O-at lower concentrations (X. M. Li et al., 2009; J. Yang et al., 2016). Iron-rich mine wastes can contain iron oxides and co-occurring hydroxysulphates due to their presence in the parent ore (e.g., lateritic deposits and gossans) (Freyssinet et al., 2005; Marsh & Anderson, 2011; Sillitoe & Perelló, 2005). Alternatively, these minerals can also occur because of subsequent subaerial weathering of iron-bearing minerals, especially iron sulphides, in mine site precipitates (used in the current study) and mine water treatment residues of which multimillion tonne arisings are produced annually (e.g., Mudd & Boger, 2013). Associated elements of value are derived from the same parent ore and may be relatively enriched in the wastes, mine water and/or resultant precipitates (e.g., Royer-Lavallée et al., 2020; Vaziri Hassas et al., 2020).

Iron-rich wastes therefore comprise a large technospheric stock of iron and associated valuable elements and as such will likely become a promising target for resource recovery. The target of value recovery might conceivably be the iron or the other associated elements of value, or both. As well as an iron source for steel making, iron oxides once decontaminated to acceptable levels can find diverse applications including being used as pigments (Hedin, 2003; Legodi & de Waal, 2007; Ryan et al., 2017), ferrites (e.g., Novais et al., 2016; Tamaura et al., 1991; Wang et al., 1996), and water/wastewater treatment reagents (e.g., Sapsford et al., 2015; Xu et al., 2012; Zhong et al., 2006).

To date, studies into metal recovery from iron-rich wastes and ores have been largely focused on abiotic leaching (e.g., Das et al., 1997; Hernández et al., 2007). Biohydrometallurgical and biomining technologies hold promise for sustainable resource recovery from wastes, by reducing the energy and reagent usage (and hence carbon intensity) associated with conventional hydrometallurgical and pyrometallurgical processes. Existing biohydrometallurgical leaching (applied *in situ* or *ex situ*) are already extensively used in

processing of sulphidic ores. Other proposed biomining approaches include the use of other acids, cyanogenic, or chelate-generating microorganisms to mobilise metals (Lee & Pandey, 2012). Bioreduction of iron oxide, where the oxidation of a suitable electron donor is coupled with the reduction under anaerobic conditions of Fe(III), has been explored as a mechanism for metal recovery from (particularly lateritic) ores (Esther et al., 2020; Papassiopi et al., 2010). Recovery of Ni, Co, and Cu from laterites has been explored extensively using dissimilative iron reducing microorganisms (DIRM) (Hallberg et al., 2011; Ňancucheo et al., 2014; Smith et al., 2017) for ore biobeneficiation (Natarajan, 2015), but there are very few studies that focus on metal recovery from wastes. To date, DIRM utilised in most biohydrometallurgy studies are specifically cultured and supplied with an optimal carbon source, nutrients, and conditions for growth, with all the commensurate implication for carbon intensity and costs should these *ex-situ* bioreactor processes be upscaled.

This paper focusses on the bioreduction of Fe(III) oxide/hydroxysulphate-bearing mine waste in the context of *in situ* biostimulation, and the potential impact of this biostimulation on resource recovery from wastes. It was hypothesised that the biostimulation would be carried out by DIRM. Since DIRM are phylogenetically diverse and include heterotrophic, autotrophic, and mixotrophic microorganisms they are widely distributed in the environment. Archaeal iron reducers are found within *Euryarchaeota* (e.g., *Ferroglobus*) and *Thermoproteota* (e.g., *Sulfolobus*) (Esther, Sukla, et al., 2015; Weber et al., 2006). Bacterial iron reducers have been identified in *Firmicutes* (e.g., *Bacillus, Clostridium*), *Proteobacteria* (e.g., *Acidiphilium*, *Aeromonas*), *Acidobacteria* (e.g., *Geothrix*), and *Deferribacteres* (e.g., *Geovibrio*). The occurrence of extremophile iron reducers viz., acidophilic (Falagán & Johnson, 2014), alkaliphilic (Fuller et al., 2015), thermophilic (Zavarzina et al., 2007), and halophilic species (Pollock et al., 2007) are further promising for biotechnologies involving IMWs which can present "extreme" environmental conditions.

DIRM are able to utilise a range of organic and inorganic electron donors (D. Lovley, 2013) including glycerol (Hallberg et al., 2011; X. M. Li et al., 2009), lactate (Chen et al., 2018; Zachara et al., 2001), acetate (Eusterhues et al., 2014; Lonergan et al., 1996; Vaxevanidou et al., 2015), pyruvate (Straub et al., 1998; Y. Xu et al., 2014), yeast extract (Greene & Sheehy, 1997), emulsified vegetable oil (Dong et al., 2017), humic acid (Stern et al., 2018), ethanol, butanol, and propanol (Straub et al., 1998), ammonium (Ding et al., 2017; Shuai & Jaffé, 2019), hydrogen (Caccavo et al., 1992; Vargas et al., 1998), and sulphur (A. Das et al., 1992; Osorio et al., 2013). Some of these meet the requirement of a potentially abundant low- or zero-cost electron donor using an industrial symbiosis-inspired solution involving waste. In this study glycerol was used, which is a cheap organic carbon source produced in large quantities as a waste by-product of the biodiesel industry (Yang et al., 2012). Worldwide production figures of which were ~47 million m^3 in 2019 (*International - U.S. Energy Information Administration (EIA)*, n.d.). One kilogram of glycerol is formed per 10 kg and as such circular/industrial symbiosis routes to utilisation of the glycerol is

of importance to this burgeoning industry (Zhang et al., 2022). Utilising this to treat mine waste would mean using one kind of waste to treat another, and may negate any costs (Ciriminna et al., 2014).

For the iron hydroxysulphate minerals jarosite ($KFe^{3+}_3(OH)_6(SO_4)_2$) and schwertmannite ($Fe_{16}O_{16}(OH)_y(SO_4)_z \cdot nH_2O$), the presence of structural sulphate presents an indirect route to iron reduction via reaction with sulphides produced by microbial sulphate reduction. Iron oxyhydroxides are highly reactive with respect to dissolved sulphide, the reaction producing FeS and elemental sulphur directly or ferric sulphide that can disproportionate to pyrrhotite/pyrite and elemental sulphur. The majority of literature focuses on Fe(III) bioreduction within the iron hydroxysulphate structure (Bingjie et al., 2014; Castro et al., 2013; Jones et al., 2006; Smeaton et al., 2012) but bioreduction of structural sulphate to sulphide within iron hydroxysulphates has also been demonstrated (Gramp et al., 2009; Ivarson et al., 1976).

This study uses laboratory-scale flow-through column reactors to examine the effect of using glycerol (10% w/w) to stimulate the *in situ* microbial community in an iron oxide/ hydroxysulphate-bearing mine water precipitate to examine the impacts in terms of, evolution of microbiological community, element mobility, and subsequent hydrometallurgical extractability of metals.

2. Materials and Methods

2.1 Iron oxide/hydroxysulphate-bearing waste sampling and characterisation

Material was sampled from the Parys Mountain legacy Cu mine, located ~2.5 km south of Amlwch in Anglesey, North Wales (53°23'13 N, 4°20'37 W). Samples were obtained from former copper cementation pond, now infilled with ochreous sediment, to the south of the site (Fig.1). The material (Parys Mt.) was homogenised manually and left to settle for 48 hrs, after which excess water was decanted and stored at 4°C. Post this, the sample was manually homogenised again for 10 mins by continuously stirring and folding within a bucket, left to settle for 1-hour, and the supernatant discarded. After repeating this procedure, samples were taken aseptically, for mineralogical, chemical, and microbiological characterisation. Measurements of the dry solids content (% weight), bulk density, dry density, void ratio, particle size distribution, and specific gravity were performed in accordance with BS 1377-2:1990. The particle size distribution (PSD) of the -150 μm sieve fraction was characterised with a Mastersizer 3000 laser diffraction particle size analyzer (Malvern).

Chemical characterisation was undertaken on the Parys Mt material before and after column experiments. The waste was dried in an oven (105 °C) for 24 h. Approximately 0.15 g sample was digested in 6 ml aqua regia in a PTFE-lined ceramic vessel using a microwave digestor (Multiwave 3000 Anton Parr). The

digested samples were analysed using an inductively coupled plasma- optical emission spectroscopy (ICP-OES; Perkin Elmer Optima 2100). The pH of the wastes was measured using the paste pH methodology outlined in BS ISO 10390:2005, with Mettler Toledo InLab™ Expert Pro pH probe. Mineralogical characterisation was undertaken using fine powder X-ray diffractometer (XRD; Philips PW3830 X-ray generator, PW1710 diffractometer controller) with a cobalt (Co Kα) or copper (Cu Kα) radiation source, scan angle range of 2θ from 5° to 90°, a step size of 0.02°, and scan step time of 0.5 s. The traces were analysed using the mineral database software, X-pert Hi Score plus analysis. Total carbon and sulphur analysis of the solid waste samples was performed using a Leco SC-144DR furnace. Total carbon (TC) and Total Organic carbon (TOC) were analysed using a Shimadzu SSM-5000A. Total inorganic carbon (TIC) was calculated by difference (TC – TOC) after phosphoric acid pre-treatment and analysis.

A sequential extraction procedure adapted from (Poulton & Canfield, 2005), designed for iron rich sediments, was used to differentiate various phases. These phases are ascribed as carbonate associated iron (Fe_{Carb}); easily reducible oxides (Fe_{ox1}) e.g., ferrihydrite; reducible oxides (Fe_{ox2}) e.g., goethite and haematite; magnetite (Fe_{mag}); and residual fractions (Fe_{res}). Metal concentrations within each fraction was determined by ICP-OES. Initial extraction with deionised water was used to account for any metal present in the water-soluble phase (Fe_{wat}). See table 1 for details.

Table 1 Summary of the sequential extractions used for iron rich sediments

Target Phase	Extractant Used	Extraction Condition
Water soluble (Fe_{wat})	Deionised water	1 h, RT
Carbonate phases (Fe_{carb})	1 M sodium acetate solution acidified to pH 4.5 with 99% acetic acid	24 h, RT
Easily reducible oxides (Fe_{ox1})	1 M hydroxylamine hydrochloride with 25% (v/v) acetic acid	48 h, RT
Reducible oxides (Fe_{ox2})	50 g/l sodium dithionate solution buffered to pH 4.8 with 0.35M acetic acid/0.2M sodium citrate	2 h, RT
Magnetite phase (Fe_{mag})	0.2M ammonium oxalate/0.17M oxalic acid solution	6 h, RT in dark
Residual fractions (Fe_{res})	Aqua regia. 50/50 solution of 65% nitric acid and 37% hydrochloric acid	42 min in microwave; 25 min cooling time

RT- room temperature

2.2 Column experimental set-up

Three sets of triplicate up-flow reactors were packed with: (i) unadulterated waste, to be later fed with 10% w/w glycerol in deionised water (DIW) (live); (ii) autoclaved waste fed with 10% w/w glycerol in DIW

(autoclaved); and (iii) unadulterated waste fed with DIW (organic starved). Columns were constructed from 1 L high density polyethylene (HDPE) bottles fitted with an inlet/outlet valve at either end. Each bottle was washed 3 times with DIW and autoclaved before use. Column effluents were collected in 2 L Erlenmeyer flasks which had been purged with nitrogen and fitted with a 2-hole rubber bung. One hole was for the inflow tube from the column whilst the other was fitted with a brewer's airlock "bubbler" valve to limit ingress of air to the collection flask (Supplementary Figure 1). Columns were fed at a flow rate of 0.2 ml/min, using a Watson Marlow 205U peristaltic pump, giving a nominal residence time of ~ 25 h. Effluent samples were collected at 2–3-day intervals and physicochemical parameters were measured. Subsamples acidified with 20% (v/v) HNO_3 were stored in the refrigerator at 4 °C until analysis. The experiments were run for 91 days. Iron oxide staining was noted in some collection vessels. This was recovered by an acid wash (37% HCl), with subsequent determination of metals (Section 2.3). After column decommissioning, sludge was extracted from the columns and subsampled for further analysis.

2.3 Analysis of Effluents

Analysis of pH, oxidation reduction potential (ORP), electrical conductivity (EC), and dissolved oxygen (DO) were measured using calibrated Mettler Toledo probes: InLab™ Expert Pro pH and ORP-probes, LE703 conductivity probe, 605-ISM DO probe in conjunction with a Mettler Toledo SevenExcellence™ Multiparameter system. Effluent alkalinity was measured using a Hach 16900 digital titrator. Elemental (Fe, Cu, Pb, As, Zn, Al, Ni, and S) analyses were conducted by ICP-OES (Perkin Elmer Optima 2100 DV). Colourimetery (HACH DR900) was used for the determination of Fe(II) (phenanthroline method) and sulphate concentrations (SulfaVer® 4 turbidimetric method). Glycerol concentrations were measured in column influents and effluents using a fluorometric free glycerol assay kit (Sigma Aldrich, Gillingham, UK) and Infinite® F50 fluorometer with Magellan software.

2.4 Hydrometallurgical Extractions

The pre- and post-experiment column material were subjected to leaching using either hydrochloric acid (HCl), sulphuric acid (H_2SO_4) or citric acid ($C_6H_8O_7$) at concentrations of 1 M, 0.5 M and 0.25 M (cf. (Esther, et al., 2015)) or 10 mM, 5 mM, and 2.5 mM of ethylenediaminetetraacetic acid (ETDA), amended to pH 8 with NaOH (cf. (Sun et al., 2001)). All tests were performed in duplicates at L:S of 10:1 on an orbital shaker (24 h at 120 rpm) within a glovebox under N_2. Final extracts were filtered through a 0.2 μm cellulose acetate filter and analysed by ICP-OES for Fe, Zn, Pb, Al, Cu, As, and S. To quantify the impact of glycerol on the leachability of metals, additional tests were performed on pre-experiment wastes where 10 mM of glycerol was added to the lixiviant (Supplementary section 1.1). The presence of glycerol was shown to have no effect on the subsequent leachability.

2.5 Microbial community analysis:

Total DNA was extracted from both the pre- and the post-experimentation waste using the Fast DNA® SPIN Kit for Soil (MP Biomedicals, Solon, OH, USA) as per manufacturer's instructions, with slight modifications according to (Webster et al., 2003). Qubit dsDNA assay kit (Invitrogen, Carlsbad, CA, USA) was used to quantify the extracted DNA. Next-generation sequencing (NGS) of bacterial and archaeal 16S rRNA genes and analysis was done as described in (Srivastava et al., 2022).

3. Results and discussion

3.1 Physicochemical characterisation of the Parys Mountain waste:

The Parys Mt. material was well graded with a range of particle sizes present (Supplementary Figure 2a, b). 58.2% of the mass of the waste was of gravel size or greater. These larger particles largely comprised of quartz, silicates, and highly weathered iron-rich gossan. 34.3% of the waste comprised of sand sized particles and 7.57% of the waste was silt or clay. The 150 µm sieve material ranged from 2.4 µm (D_{10}) to 94 µm (D_{90}), with a D_{50} of 11 µm. Parys Mt. waste was acidic (pH = 2.61), with a sulphur content of 3.08 wt.% and an organic carbon content of 0.68 wt.%. Table 2 shows the physicochemical properties of the waste. Metals of potential economic interest within the waste include Pb (0.27%), Zn (0.17%), and Cu (0.69%). XRD analysis indicated the presence of quartz, jarosite, and goethite, correlating with the high Fe, S, and K concentrations found by total digest and Leco sulphur analysis (Supplementary Figure 2c).

Table 2 Physicochemical characteristics of the Parys Mountain waste

Property	Value
Solids content	73.49 ± 2.01 wt %
Bulk density	1.71 ± 0.15 g/cc
Dry density	2.55 ± 0.07 g/cc
Specific gravity	3.08 ± 0.15
Void ratio	1.82 ± 0.19
Paste pH	2.61 ± 0.07
Sulphur	3.08 wt %
Total carbon	0.68 wt %
Inorganic carbon	0 wt %
Total organic carbon	0.68 wt %

Supplementary Figure 2d shows the distribution of Fe throughout the sequential extraction phases present in the waste. A minor proportion of iron was present in the two most reactive phases, viz., carbonate associated (carb), and easily reducible oxide (ox2). 40.9% of the reducible oxide phase (ox1) comprised of Fe. Zn, like Fe, was also found mostly within the 3 least reactive phases (Supplementary Figure 2d). The

largest of these phases is the residual phase (res) with 47.8% total Zn. 6.4% and 1.4% of total Zn was located within the carbonate associated, and easily reducible oxide phase. 23.2% of total Zn was held within the reducible oxide phase while the remaining 21.3% was within the magnetite targeted extract (mag). Over half of the Pb was located within the magnetite targeted extract (54.1%) while a further 29.5% was located within the residual phase. The remaining 16.4% of total Pb was distributed between the three most reactive phases, which represent target phases for metal recovery via microbial reductive dissolution of iron. The relatively low amount of Pb within these target phases suggests that there is significantly less Pb associated with iron oxyhydroxides (either co-precipitated or absorbed) or as easily leachable minerals. Although a greater amount of Pb was present within the waste it appears that a lower proportion of this waste may be available for recovery via reductive dissolution.

The distribution of Cu was like Pb where most of the Cu was held within the magnetite targeted (46.9%) and residual (46.5%) phases. Despite the elevated Cu concentrations within the waste, the sequential extraction results suggest that only minor quantities of Cu are likely accessible for recovery as only 3.1% and 3.5% of total Cu was contained within the carbonate associated and easily reducible oxide phases respectively. It is notable, however, that no Cu was extracted in the reducible oxide phase representing crystalline ferric oxides such as goethite. This is attributable to the sodium dithionite within this phase's extractant which causes solubilised Cu to precipitate out of solution (Chou et al., 2015). This effect causes Cu to be underrepresented in the reducible oxide phase and therefore potentially overrepresented in the subsequent phases. This makes predicting the amount of Cu that can be considered feasibly recoverable difficult and inaccurate (Chou et al., 2015).

Despite higher concentrations of the primary target metals of Zn, Pb, and Cu within the waste, sequential extraction data suggests that a smaller proportion of this metal value is potentially recoverable by reductive dissolution of iron. If conservative recovery targets, using only the easily reducible oxide and reducible oxide phases, are considered then ~24.5% Zn, ~13% Pb, and ~3.5% Cu can be considered feasibly recoverable.

3.2 Column effluent chemistry:

3.2.1 Iron release and pH/ORP/EC

Figure 2 shows the total Fe release and corresponding pH/ORP/EC for the column experiments. Fe was released from all columns but showed markedly different behaviour. The organic starved column (control) demonstrated that iron was leaching from the column in response to water flushing. The results indicate a typical flush curve suggesting that there is a pool of soluble iron (some of which is clearly Fe(II) – see

Figure 3a) that was being mobilised and removed from the column in response to water flushing, this is also supported by the decrease in EC with time (Figure 2a). The proportion of Fe(II) did not increase with time. The pH (Figure 2a) was around pH 3 reflecting the paste pH of the material and explaining the presence of soluble iron in the effluent, which later increased gradually to ~ pH 6.5. The ORP remained consistent at a value 420 mV ±25 mV. DO was 5.44 mg/l which dropped to negligible indicative of anaerobic conditions in the column. The behaviour of the organic starved material contrasts with the columns where glycerol was introduced (Figure 2 & 3).

Total Fe (Fe_{Tot}) concentrations in the live columns were much higher (369 mg/l on day 91) than that observed in control (101 mg/l on day 91), suggesting that addition of glycerol lead to enhanced release of iron. It decreased steadily from the peak of 1363 mg/l on day 21 to 367 mg/l on day 56. Thereafter, Fe_{Tot} remained relatively constant until day 75, after which a further decrease was observed (Figure 3b). Fe(II) increased from day 8 onwards indicating the onset of reducing conditions and iron reduction in response to glycerol addition (Bridge & Johnson, 1998), which was not observed in organic starved controls. Thereafter, Fe(II) in these column effluents displayed a similar pattern to that of Fe_{tot} (Figure 3b). pH increased from the initial low value of pH 3.15 on day 1 to a final pH of 6.68 on day 91(Figure 2b). The increase was coeval with the rapid increase in iron concentrations, indicating the onset of iron and/or sulphate reduction as these are both protons consuming/alkalinity producing reactions (Paper et al. 2021). The variability in releases between replicate columns may be attributed to the variations in flow path/residence time. DO within the effluents was initially high, but soon dropped to <1 mg/l indicating anaerobiosis. Eh steadily decreased throughout the experiment, with the rate of decrease slowing towards the later stages of experimentation (Figure 2b). Eh was ~70 mV when the pH was circumneutral, below the critical Eh (~100mV) suggested for iron reduction (Petruzzelli et al., 2005) but above the critical Eh (-150mV) for sulphate reduction (Connell & Patrick, 1968). However, this reflects the effluent only and it is likely that a range of redox gradients existed within microenvironments of the waste.

Fe_{Tot} in the autoclaved column effluent remained constant at ~340 mg/l for around 14 days before increasing sharply (Figure 3c). Similarly, the Fe(II) concentration remained between 10-14 mg/l until day 12, after which a sharp increase was observed (Figure 2c). Autoclaving the waste led to a substantially longer "lag phase" as compared to live columns (Figure 3). Although the Fe_{Tot} exhibited an increase with time, the increase was lower than that observed in live columns; with Fe_{Tot} increasing gradually at an average rate of 27.5 mg/l/day to a peak of 791.0 mg/l on day 44 of the experiment. Unlike Fe_{Tot}, the average peak Fe(II) concentration of 400 mg/l, was far closer to the live column equivalent (Figure 3c). The solubility of Fe(II), as in the live columns, did not limit the recovery of iron from the columns. An average of 5.4% of total iron was recovered from the autoclaved columns. Both pH and alkalinity of the autoclaved column effluents increased coevally with the increase in Fe_{Tot} over time (Figure 2c) and exhibited a trend very similar to live column effluents. The significant reduction in the rate of pH increase, post-day 44 is likely a reflection of

reduced microbial activity in the columns as also evidenced by the decreasing Fe_{tot} concentrations. Autoclave resistant spores present in the waste may be responsible for the microbial activity that regulates the physicochemical parameters (O'Sullivan et al., 2015; Srivastava et al., 2022).

Eh remained constant for first 12 days, after which it decreased steadily to the end of the experiment ending at ~-70 mV (Figure 2c), just as in the live column. A simultaneous increase in both the Eh and Fe_{tot} concentration was observed, which further indicates microbial activity. DO exhibited a rapid decrease to <1 mg/l and remained so for the duration of the study indicating anaerobic conditions, ideal for microbial dissimilative iron reduction (D. Lovley, 1993; Weber et al., 2006). Similarly, EC exhibited the same trend as live columns indicating iron to be the dominant cation in the effluent (Figure 2c).

3.2.2. Sulphate

Sulphate concentration in the organic starved column effluent remained consistently at ~ 240 mg/l and exhibited a trend similar to Fe_{Tot} (Figure 3d). The SO_4^{2-} released in the other experimental column effluents fed with glycerol was higher than organic starved that can be attributed either to the SO_4^{2-} sorbed on to mineral surfaces or the dissolution of iron hydroxysulphates such as jarosites (Bridge & Johnson, 1998; Jones et al., 2006). Sulphate concentration in live column effluent exhibited a similar trend to that of Fe_{Tot} concentrations and was significantly higher than organic starved column effluents (Figure 3d). This suggests that jarosite is the target for bioreduction where, both Fe(II) and SO_4^{2-} are solubilised from jarosite, commensurately. A decrease in SO_4^{2-} concentration is observed from day 56 onwards with a concomitant increase in pH to circumneutral conditions. This may either be attributed to a decrease in jarosite bioreduction or sulphate reduction superseding iron reduction. The latter is thermodynamically favourable at circumneutral pH conditions (Chapelle et al., 2009; D. R. Lovley & Phillips, 1987). As with the Live samples, the trend in average effluent sulphate concentration is similar to the Fe_{tot} concentration within the autoclaved effluents, with a broad curve peaking at 1200 mg/l (day 42; Figure 3d). Decrease in SO_4^{2-} concentration from day 49 onwards is indicative of sulphate-reducing conditions. Iron oxides are very reactive towards HS^-, a product of sulphate reduction, reacting to form iron monosulphides (Hansel et al., 2015; Riedinger et al., 2017).

3.2.3. Release of Cu, Pb, Zn

The effect of biostimulation on the release of metals was evaluated by determining the concentrations of metals present in the column effluents (Figure 4). Organic starved control columns exhibited low recovery of Fe (1.6%), Zn (4.7%), Cu (0.7%), and Pb (0.1%). Zn and Cu exhibited an initial release typical of a 'wash off' of weakly sorbed or water-soluble fraction, however the recovery declined post day 8. Pb release

remained consistently at ~ 0.3 mg/l through the early part of the experiment, though variability was observed post day 49 onwards (Figure 4a). Live columns, on the other hand exhibited only 3.1 %, 0.3%, and 0.1 % of total Zn, Cu, and Pb, respectively. The recovery rate of metals from live columns was lower than organic starved control columns. Like in control columns, majority of the Zn and Cu were recovered in the initial wash off phase. Although minimal recovery of Pb was obtained, it exhibited a trend similar to Fe_{Tot}. Metal mobility could be limited by the increasing pH (Figure 2b) as higher pH typically leads to lower mobility of Zn> Cu> Pb (Sintorini et al., 2021). According to this, organic starved control should have exhibited a higher recovery of Zn and Cu, however it exhibited a similar low recovery as live columns, suggesting that pH did not play a role in the mobility of these metals.

Autoclaved columns exhibited a slightly higher recovery of Zn (5.8%), Cu (0.8%), and Pb (0.2%) as compared to organic starved control or live columns. As previously, majority of Zn and Cu was recovered in the early stages of the study which rapidly declined to negligible concentrations, suggesting "wash-off" (Figure 4c). The elevated metal recovery may be due to the heat sterilisation that induces the transformation of amorphous ferrihydrite (or similar) to goethite thereby reducing the surface area and its ability to adsorb associated metals (S. Das et al., 2011). Effluent Pb concentrations displayed very little similarity to Fe_{tot} trend. Pb concentrations decreased for the first 12 days, after which they exhibited an increase, peaking at 0.8 mg/l on day 16, followed by a further decrease and stabilising at ~0.1 mg/l for the remainder of the experiment. The decrease in Pb immediately after the Pb elevation on day 19, at acidic pH (3.5) of effluent, is unlikely due to the re-sorption of Pb^{2+}, as Pb^{2+} is usually soluble under acidic conditions and the surface adsorption on minerals like iron oxyhydroxides is merely ~10% (Brown et al., 2008). The lack of relationship between Fe_{Tot} and Pb in control effluent concentrations confirms the assumption that the increased concentrations observed in both the live and autoclaved columns (coeval with increasing Fe_{Tot}) is a consequence of the reductive dissolution of iron hydroxysulphates in the waste. It also supports the theory that the decline in Pb within these effluents is a result of increasing pH as Pb is observed to remain relatively constant in the control effluents which also exhibit a stable pH.

3.2.4 Glycerol utilisation

Glycerol was added as an additional carbon source in the live columns. Influent of the live columns contained 10 mM glycerol (Figure 5). Concentrations of glycerol in the first few days remained between ~4.5 mM and ~6.5 mM, however, from day 12 onwards it decreased to ~1 mM and remained until the end of the experiment. This is accompanied by a concomitant increase in iron concentrations suggesting microbial activity. This also suggests that the amount and/or rate of supply of glycerol could have been increased, an important area for further investigation and consideration for upscaling. The total glycerol added over the column test was 0.027 kg per kg of Parys Mt.

3.3 Visual, chemical, and mineralogical characterisation of post experiment waste

The Parys Mt. waste, which was originally orange-light brown in appearance, post experiment largely changed to olive-khaki green in colour. The cross-section of the column (Supplementary Figure 3) exhibited variability with light brown regions in the centre demonstrating the impact of preferential flow paths within the waste with discrete areas undergoing less extensive bioreduction. This would inherently limit the amount of target metal that could be extracted by the flow of extractant and in the latter hydrometallurgical extractions.

Mineralogical characterisation was done by XRD. The Parys Mt. waste exhibited characteristic peaks of quartz, jarosite, and goethite, which after being fed with organic starved influent post-experiment still exhibited a similar diffractogram (Supplementary Figure 2c). However, live column waste post-experiment exhibited differences from pre-experiment waste, most significant being the absence of ~34.2 °2θ peak corresponding to jarosite (Supplementary Figure 2c) suggesting the utilisation of jarosite as primary electron acceptor for DIRM. Both biotic and abiotic reduction of iron oxyhydroxides and hydroxysulphates result in generation of iron sulphides (Y. L. Li et al., 2006; Riedinger et al., 2017). However, peaks corresponding to FeS were absent which may be attributed to their metastable nature and susceptibility to rapid oxidation (Rickard & Morse, 2005). Heat sterilisation of the Parys Mt. waste resulted in a slight modification of the X-ray diffractogram with two additional peaks observed at ~43 °2θ and ~59 °2θ, corresponding to lepidocrocite. Post- experiment autoclaved waste XRD data was very similar to live post experiment waste.

Sequential extractions of organic starved waste exhibited very little redistribution of metals pre- and post-experiment (Figure 6a). A small amount of redistribution of Fe to reducible oxide (36.1%) and easily reducible oxide (11.1%) phase was observed (Figure 6a). Zn exhibited negligible changes in the various extractive phases with very little redistribution to easily reducible oxide (5.7%), reducible oxide (17.5%) and residual (63.6%) phases. A small amount of Cu redistributed from residual and magnetite targeted phases to more reactive phases viz., easily reducible, and reducible phases (Figure 6a). Pb on the other hand exhibited a minor redistribution from water soluble, carbonate, and easily reducible oxides phases to magnetite targeted and residual phases (Figure 6a). The most notable change was the decrease of Pb proportion in the carbonate associated phase from 9.4% to 2.5%, suggesting the mobilisation of Pb to aqueous phase, however, <0.1% lead was recovered from the aqueous phase, indicating redistribution to least reactive phases. Similarly, very little redistribution of Fe was obtained (Figure 6b) in live columns post experiment, despite the apparent bioreduction observed during effluent analysis. Most of the Fe post experiment was held in the least reactive magnetite-targeted (18.3%) and residual phases (48.2%). Unlike

Fe, Cu redistributed from least reactive phases (res and mag; Figure 6b) to more reactive phases (carb and ox1; Figure 6b). Although the redistribution of Zn in post experiment live columns was only minor, the trend was similar to Cu. Pb exhibited most extensive redistribution from least reactive phases to more reactive phases with more than 50% present in the easily reducible oxide phase.

Autoclaving of Parys Mt. waste did not have a significant effect on the distribution of Fe, Cu, and Zn between sequential extraction phases when compared to live pre-experiment waste, except for Pb (Figure 6c). Steam under pressure resulted in redistribution of Pb from more reactive phases to least reactive phases with majority of Pb partitioning into the residual (69.4%) phase. Fe distribution in post-experiment autoclaved columns was similar to their live counterparts, with majority of Fe being in the residual (45.3%), reducible oxide (27.4%), magnetite targeted (10.8%), and easily reducible oxide (8.1%) phases, in that order. Despite the lower Fe concentrations in the effluents from autoclaved columns, the impact of bioreduction in the live and autoclaved columns seem to be comparable as evident from the similarity of distribution within various phases. Bioreduction resulted in minor redistribution of Zn from residual phase to magnetite targeted (16.3%), reducible oxide (16.5%), and easily reducible oxide (7.3%). Although slight, an apparent increase in carbonate associated (1.9%) and water-soluble (2.4%) phases was also observed. Cu was predominantly present in the magnetite targeted (63.5%) and residual (24.6%) phases, which post-experimentation got redistributed to more reactive easily reducible oxide (22.5%) while majority remained within the residual phase (59.8%). Furthermore, just like Cu, an increase in carbonate associated (5.9%) and water soluble (5.6%) phases was observed. Pb redistribution in the post experiment autoclaved waste occurred from least reactive phase (res- 69.4%) to more reactive phases (ox1- 49.5%; carb- 25.8%), because of biostimulation/bioreduction. This is similar to the trend exhibited by the live column.

3.4 Microbial Community Analyses

Bacterial and archaeal 16S rRNA gene sequences generated by next generation Illumina sequencing were used to identify and characterise microbial communities within the wastes, both pre-and post-experiment. Sequences were classified from phylum to genus level and quantified by their relative abundance. A total of 14 different phyla were identified in the original waste sample, consisting of 12 bacterial phyla and 2 archaeal phyla (Figure 7a). Of these, 10 of the bacterial and archaeal phyla were present at ≥1%. Interestingly, there was no single phylum that clearly dominated the system with *Planctomycetes* being the most abundant at 23.9%, followed by *Firmicutes* (16.3%) and *Proteobacteria* (14.1%). Classes *Bacilli* (10.1%) and *Clostridia* (6.2%) represented the entirety of the *Firmicutes* while *Alphaproteobacteria* (4.9%) and *Gammaproteobactaria* (8.4%) represented the majority of the *Proteobacteria*. Figure 7a shows all the bacterial phyla identified in pre-experiment samples.

In total 21 known cultured genera were identified in Parys Mt. waste, of which 3 were from the domain Archaea (Figure 7b). Many of the genera identified comprised of uncultured bacteria or archaea of higher order or classes. Of the known cultured genera identified, *Acidobacillus* (10.0%) was the most abundant, which are acidophilic bacteria known for both iron-oxidation and reduction and have been identified in acid mine drainages (AMD) (ñancucheo et al., 2016; Shiers et al., 2016). Members of this genera have also been used for recovery of Cu from mine tailings (Falagán et al., 2017) and Co from limonitic ores (Smith et al., 2017). Amongst the other genera present in relatively low abundances, species within *Leptospirillum* are known to oxidise iron (Ojumu et al., 2009), while those present in *Desulfosporosinus* (Spring & Rosenzweig, 2006), *Acidiphilium* (Falagán & Johnson, 2014), *Metallibacterium* (Ziegler et al., 2013), and *Acidibacter* (Falagán & Johnson, 2014) are known to be iron reducers. Previous studies on Parys Mt. waste had identified *Leptospirillum spp.* in the surface spoils (Bryan et al., 2004) and *Acidiphilium* in the AMD contaminated Afon Goch area (Jenkins et al., 2000). However, *Acidithiobacillus*, *Thiobacillus*, and *Ferromicrobium,* identified in the previous study were not identified in the present study, which indicates that the waste investigated here has a microbial community distinct from the ore body of the AMD.

The microbial community composition of the organic starved columns exhibited a slight difference from pre-experiment samples. *Planctomycetes* exhibited an increase in relative abundance from 23.9% to 42.8%, on the other hand, *Cyanobacteria* and *Firmicutes* decreased in relative abundance (Figure 7a). Within *Planctomycetes* uncultured bacterium belonging to *CPLa-3 termite group* was the predominant genus, exhibiting an increase from 18.5% to 40.7% (Figure 7b). Other bacterial genera were present at low abundances of 4.0% or less. As expected, given the lack of iron reduction in the effluent analysis, iron reducing genera were not identified.

Substantial changes were observed in the microbial community structure post-experiment in the live columns waste. *Planctomycetes* and *Proteobacteria* decreased significantly while *Firmicutes* became the predominant phyla (Figure 7a). Similarly, at the genus level, 13 genera were identified of which 5 were present at ≥1% in the pre-experiment samples, while the other 8 increased in abundance from <1% in the pre-experiment samples (Figure 7b). *Methanosaeta* was the only archaeal genera present at >1% abundance. The predominant bacterial genus identified was *Desulfosporosinus*, members of which are strictly anaerobic and form endospores (Spring & Rosenzweig, 2006). This genus and *Delsulfitobacterium* (Villemur et al., 2006), also identified here, are known for their ability to reduce both Fe(III) and SO_4^{2-}, with the latter forming H_2S and resulting in indirect reduction of Fe(III) (dos Santos Afonso & Stumm, 1992; Roberts et al., 2020). The second most abundant genus identified was *Thermincola,* below detection in pre-experiment samples, whose members are thermophilic, anaerobic, iron reducers, with very few cultured species.

Sequence analysis of pre-experiment autoclaved samples identified 9 bacterial phyla and no archaeal phyla (Figure 7a). Of the 9 bacterial phyla, only 5 were present at a relative abundance of ≥1%, which is lower than that observed in non-autoclaved pre-experiment samples. *Proteobacteria* (82.9%) was the predominant phylum (Figure 7a), followed by *Firmicutes* (12.0%), *Choloroflexi* (1.5%), *Actinobacteria* (1.4%), and *Planctomycetes* (1.3%). Both *Planctomycetes* and *Choloroflexi* exhibited a substantial decrease as compared to non-autoclaved pre-experiment waste samples. Within *Proteobacteria, Gammaproteobacteria* (76.8%) was the most abundant class, followed by *Alpha-* (2.9%) and *Beta-* (3.2%), and *Deltaproteobacteria* (<1%). *Bacilli* (5.0%) and *Clostridia* (6.9%) were the predominant classes within the phylum *Firmicutes*. At the genera level (Figure 7b) *Gammaproteobacteria* was represented by *Escherichia/Shigella* (68.7%), which is surprising as they were only identified in the pre-experiment autoclaved samples. Although there are reports of *E. coli* surviving the process of heat sterilisation (Markova et al., 2010), its presence is more likely a result of contamination of these low DNA samples by heterologously expressed commercial *Taq* polymerase (Rochelle et al., 1992) as some negative PCR controls also exhibited the presence of these genera. Within the phylum *Firmicutes*, *Desulfosporosinus* (4.5%) was the most abundant genus, followed by *Acidibacillus* (2.4%), *Clostridium sensu stricto 12* (1.7%), and *Bacillus* (1.5%), highlighting the abundance of heat-resistant spore forming bacteria in these samples (Cho & Chung, 2020; Gupta & Gao, 2009).

The addition of glycerol to the autoclaved waste resulted in significant changes in the microbial community structure of the waste (Figure 7) and showed some resemblance to the community structure observed in post-experiment live samples. The most obvious similarity in these samples is the dominance of the phylum *Firmicutes*. This phylum exhibited 6.5 times increase in abundance in post-experimental samples (78.8%) as compared to pre-experimentation autoclaved samples (12.0%). This was accompanied with a concomitant decrease in the abundance of *Proteobacteria* and an increase in *Synergistetes,* which was below detection in pre-experiment autoclaved samples. A similar effect of autoclaving was observed with iron oxyhydroxide waste fed with glycerol during a study on passive bioremediation of dye bearing effluents, in which the abundance of *Firmicutes* increased and *Proteobacteria* decreased post-experiment (Srivastava et al., 2022). Interestingly, *Euryarchaeota* exhibited an increase in relative abundance to 8.9% from below detection (Figure 7), and sequences were related to members of the sulphur reducing genus *Thermoplasma* (Bonch-Osmolovskaya, 1994). Of the 12 recognised genera present at relative abundance ≥1% pre-experiment, only 9 of these remained in post experiment. As observed in post-experimentation live samples, *Desulfosporosinus* was the predominant genus in post-experiment autoclaved samples, exhibiting an increase to 62.1% from an initial 4.5%. Other genera observed at abundance >1% were *Alicyclobacillus* (6.1%), *Desulfitobacterium* (4.5%), *Acidibacillus* (2.4%), and *Escherichia/Shigella* (1.2%). Except for *Escherichia/Shigella,* all other genera represent potential iron reducers. These spore-

forming, iron and sulphate reducing bacteria explain the observations of iron reduction in autoclaved waste and the olfactory identification of hydrogen sulphide generation during experimentation.

3.5 Hydrometallurgical Extractions

3.5.1 Hydrochloric acid leaching

The leachability of Fe from post-experiment organic starved control waste was negligible with only 2.8%, 1.2%, and 0.6% Fe leached when 1 M, 0.5 M, and 0.25 M HCl were used, respectively (Figure 8a). This is indicative of the lack of biostimulation and transformation of amorphous minerals to more crystalline phases. Bioreduction that occurred in live and autoclaved columns resulted in a slight increase in leachability of Fe as compared to pre-experiment and control column wastes. Approximately 4.2% iron was recovered from live waste post-experiment when leached with 1 M HCl (Figure 8a), and the amount of leachable Fe decreased as: 1 M>0.25 M>0.5 M. Although 1 M HCl gave the highest yield of Fe from live column wastes, 0.5 M, and 0.25 M HCl resulted in a more substantial increase in Fe recovery as compared to pre-experiment waste (Figure 8a). Autoclaving led to a small increase in the leachability of Fe from the waste when compared to pre-experiment waste, with 1 M HCl leaching ~4.7% Fe. Post-treatment autoclave waste when leached with 1 M HCl exhibited a slight decrease in the total Fe yield. However, an increase in yield was observed when 0.25 M and 0.5 M HCl were used as extractants, suggesting an increase in readily leachable phases of Fe.

The leachability of Zn from the waste before treatment was lower than that observed for Fe (Figure 8a). When compared to pre-treatment waste leachability, organic starved wastes exhibited a marginal increase in leachability by 1 M and 0.5 M, while 0.25 M had a negligible effect on the leachability of Zn. Post biostimulation, Zn leachability in 1 M, 0.5 M, and 0.25 M HCl increased to ~7.1%, 6.4%, and 5.9% respectively. Interestingly, from the perspective of processes economics, the highest recovery was obtained with 0.25 M HCl exhibiting an 8-fold increase in leachability. Autoclaving led to a slight increase in leachability of Zn in pre-experiment wastes. A 5-fold increase was observed in Zn leachability of post-experiment autoclaved wastes in response to 0.25 M HCl (Figure 8a).

Leachability of Cu from waste followed the same trend as Zn and Fe. Negligible Cu was recovered from pre-treated waste in response to HCl leaching. Post-treatment organic starved waste exhibited a non-significant increase in Cu leachability (Figure 8a). However, biostimulation substantially increased the leachability of Cu with a 15-fold increase in recovery for 0.25 M HCl (Figure 8a). The majority of Cu is readily leachable by dilute acids as Cu is redistributed from recalcitrant mineral to more reactive phases. A minor increase in leachability of Cu from pre-treatment waste was observed in response to autoclaving.

However, post-experiment autoclave wastes exhibit a comparable increase in Cu leachability as live columns.

Pb exhibited the highest leachability amongst all the metals, in response to HCl leaching. 9.3%, 4.0%, and 2.0% Pb was recovered from pre-treated waste when 1 M, 0.5 M, and 0.25 M HCl were used as lixiviants, respectively. Absence of any microbial activity in organic starved columns resulted in a minimal increase in leachability of Pb (Figure 8a). However, post biostimulation a significant increase in Pb leachability was obtained with 0.25 M HCl giving the highest recovery rate (34.73%), followed by 0.5 M HCl (30.9%) and 1 M HCl (29.9%). Autoclaving pre-experiment waste exhibited a substantial increase in Pb leachability than any other metals, which increased further post-experiment because of bioreduction and glycerol addition (Figure 8a). The results of Pb recovery of post-experiment autoclaved waste are comparable with their live waste counterparts.

3.5.2 Sulphuric acid leaching

H_2SO_4 leaching resulted in higher Fe recovery than HCl, with the pre-test waste exhibiting 5%, 3.4%, and 2% Fe recovery from 1 M, 0.25 M, and 1 M H_2SO_4, respectively. Organic starved columns exhibited low leachability of Fe (Figure 8b) due to lack of biostimulation as discussed above. However, Fe recovery for live biostimulated waste increased to 7.3%, 6%, and 5.1% when leached with 1 M, 0.25 M, and 1 M H_2SO_4, respectively. Contrary to HCl leaching results, autoclaving had negligible to marginal increase in Fe recovery for pre-test material. However, post-test the leachability increased, albeit slightly lesser than live samples (Figure 8b).

Although leachability of Zn with H_2SO_4 from the wastes exhibited a similar trend to that of Fe, the recovery is higher than for HCl leaching (Figure 8b). In organic starved samples leached with H_2SO_4, like HCl, an increase in Zn recovery when compared to pre-experiment was observed. Zn recovery from live samples was found to increase from 1.5%, 1.1%, and 1.0% in the pre-test material, to 7.9%, 6.9%, and 6.8% post-test, when 1 M, 0.5 M, and 0.25 M H_2SO_4 was used respectively. As discussed previously, lack of microbial activity in the organic starved columns resulted in lower recovery of Zn as compared to their live counterparts. Autoclaving the pre-experiment waste exhibited a marginal increase in Zn leachability, which post-experiment showed a further increase because of bioreduction.

In contrast to Fe and Zn, the leachability of Cu generally decreased in pre-experiment waste with 1%, 0.6%, and 0.5% total Cu recovered with 1 M, 0.5 M, and 0.25 M H_2SO_4, respectively. Organic starved waste exhibited a slight increase in Cu recovery (Figure 8b), which further increased with the addition of glycerol in live samples. All the three concentrations of H_2SO_4 gave almost the same recovery (~9.0%), suggesting that Cu partitioned into more reactive phases making it readily leachable by dilute acids.

Autoclaving the pre-experiment sample resulted in a minor increase in Cu leachability (Figure 8b), which post-experiment exhibited a substantial increase in recovery and is comparable to live counterparts. Pb recovery across all samples was minimal (~0.5%) and the concentration of lixiviant did not have any effect on the recovery, due to the inability of cold H_2SO_4 to solubilise Pb and formation of insoluble $PbSO_4$ (Thornton et al., 2001).

3.5.3 Citric acid leaching

$C_6H_8O_7$ is a weaker acid than HCl and H_2SO_4, and thus the recovery of metals from $C_6H_8O_7$ leaching is lower than that obtained by the other inorganic acids. Although $C_6H_8O_7$ is a known chelator of Fe in aqueous solutions, while other organic acids are not (Silva et al., 2009), the recovery of Fe from pre-experiment waste was lower than that achieved by HCl and H_2SO_4 leaching (Figure 8c). Organic starved control exhibited negligible leachability of Fe by $C_6H_8O_7$. The leachability of Fe from live samples exhibited an increase, with 0.5 M $C_6H_8O_7$ leachate showing ~9-fold increase in recovery when compared to pre-experiment. Much like the other acids, $C_6H_8O_7$ leaching of autoclaved pre-experiment waste exhibited an increased recovery yield, with ~1.0% recovered regardless of lixiviant concentration (Figure 8c). In comparison to this, Fe leachability of post-experiment autoclaved waste showed an increase, but a decrease in recovery relative to live samples. Leachability of Zn from $C_6H_8O_7$ leached pre-experiment waste was almost negligible and remained so even after experiment for organic starved waste. Bioreduction in live columns increased the recovery of Zn to 4.3% 3.8%, and 3.6% in response to 1 M, 0.5 M, and 0.25 M $C_6H_8O_7$, respectively. Interestingly, autoclaved pre-experiment waste did not show any change in leachability of Zn, which contrasts with the general trend of enhanced leachability observed for other metals and/or lixiviants used. Post-experiment autoclaved samples exhibited an increase in recovery of Zn because of bioreduction, however the yield was lower than that obtained from live samples.

As with Fe and Zn, leachability of Cu from pre-experiment waste is lower than that obtained with the inorganic acids. An increase in leachability was observed in organic starved control columns with ~1.1% recovered from all the three concentrations of $C_6H_8O_7$. Recovery of Cu exhibited a further increase in live columns to 3.4%, 2.5%, and 1.7% with 1 M, 0.5 M, and 0.25 M $C_6H_8O_7$, respectively. No significant increase in leachability of Cu was obtained on autoclaving the pre-experiment sample. However, post-experiment autoclaved waste exhibited an increase in Cu leachability that are commensurate with the live columns.

Pb, like other metals exhibited negligible leachability which demonstrates the ineffectiveness of the $C_6H_8O_7$ as a lixiviant for pre-experimentation waste. An insignificant change in recovery of Pb was observed from organic starved waste in response to $C_6H_8O_7$ leaching. However, introduction of glycerol

and subsequent bioreduction caused the leachability of Pb to substantially increase in live samples. 15.1%, 14.1%, and 9.1% Pb was recovered from live samples when 1 M, 0.5 M, and 0.25 M $C_6H_8O_7$ was used as a lixiviant, respectively. Autoclaving of the pre-experiment waste exhibited a minor increase in Pb leachability (1.8% -1 M; 1.4% - 0.5 M; 0.9% - 0.25 M), which post-experiment exhibited a significant increase to 11.6%, 11.2%, and 8.9% when leached with 1 M, 0.5 M, and 0.25 M $C_6H_8O_7$, respectively.

3.5.4 EDTA leaching

Leachability of Fe from pre-experiment wastes with the chelator, EDTA exhibited a similar trend to inorganic acid leaching, however the yield was lower (Figure 8d). 0.4%, 0.2%, and 0.2% Fe was recovered from pre-experiment wastes with 10 mM, 5 mM, and 2.5 mM EDTA, respectively. The recovery rates are commensurate with the rates obtained with $C_6H_8O_7$. Similarly, negligible recovery of Fe was obtained from organic starved waste when subjected to EDTA leaching. Live samples exhibited a slight increase in leachability of Fe however the magnitude of increase was much lower than that achieved by inorganic acids. A marginal increase in leachability of Fe was observed in autoclaved pre-experiment samples (between 0.4%-0.6%), which increased further post-experiment (between 0.9%-1.1%). The increase in leachability of Fe in pre-experiment and organic starved columns is negligible due to their acidic pH that neutralises EDTA (pH 8.0), while the live and autoclaved post-experimentation samples were circumneutral thereby facilitating extraction of Fe in EDTA. Leachability of Zn also exhibited a similar trend to $C_6H_8O_7$ leaching, with ~0.6%, 0.4%, and 0.5% total Zn recovered from pre-experiment wastes using 10 mM, 5 mM, and 2.5 mM EDTA, respectively. Organic starved waste exhibited a similar trend in Zn leachability in response to EDTA (Figure 8d). The recovery of Zn increased in live samples because of bioreduction (Figure 8d). Autoclaving exhibited an insignificant increase in leachability of Zn from pre-experimentation waste, which post-experimentation increased to ~1.8%.

Much like Fe and Zn, the recovery rates for Cu from pre-experiment waste with EDTA as the lixiviant were low (Figure 8d). Leachability of Cu in organic starved samples showed a marginal increase as compared to the pre-experiment waste. Live samples, on the other hand, exhibited an increased leachability of Cu as compared to both pre-experiment and organic starved wastes, with 6.2%, 4.9%, and 12.4% recovered with 10 mM, 5 mM, and 2.5 mM EDTA, respectively. These recovery rates are higher than those obtained with $C_6H_8O_7$. Autoclaving resulted in a negligible increase in leachability of Cu in pre-experimentation waste, which increased in post-experimentation samples, but lower than live column material. Leachability of Pb from pre-experiment waste by EDTA gave the highest yield, with 7.4%, 3.2%, and 4.2% total Pb recovered using 10 mM, 5 mM, and 2.5 mM EDTA, respectively. Organic starved samples, on the other hand, exhibited a significant decrease in leachability. Bioreduction of the waste further increased the leachability of Pb between ~29% - ~35% in live samples (Figure 8d). Surprisingly,

autoclaving the pre-experiment waste led to a decrease in leachability of Pb by 10 mM and 5 mM EDTA, which is in contrast with the leachability exhibited by EDTA for other metals, and for all metals by other acids. 2.5 mM EDTA, on the other hand, exhibited an increase in leachability of Pb when compared to its non-autoclaved pre-experiment equivalent. Much like live column material, post-experiment autoclaved column material also exhibited a significant increase in total Pb recovery (Figure 8d). In general, EDTA exhibited a high rate of Pb leachability as compared to other metals, with Pb seemingly outcompeting other metals for EDTA binding sites.

Glycerol fed wastes exhibited a higher leachability highlighting the role of microbial activity in mobility of metals. In general, Fe leaching exhibited a slight increase post-test. Zn was majorly associated with residual phases within sequential extractions which didn't appear to change, yet notable increases in extractability were observed. Similarly, most of the Cu was associated with the residual phase within the waste, however some of it was also associated with the easily reducible oxide phases which would explain the increased leachability in response to lixiviant application. Pb was associated with more reactive phases and was clearly seen to move pre- and post-test. This corresponded to release of Pb concurrently with Fe, although this was later curtailed probably due to the increasing pH of the system. This suggests if pH were maintained at lower pHs it may be possible to extract Pb directly from the waste. Even though Pb was retained at later stages of the work, the fact that had it moved phases corresponded to it responding very well in the hydrometallurgical extractions, furthermore the chelation extraction was notable in the selectivity of metal removal over Fe – important in extracting value from the waste.

Conclusions

Significant changes in waste colouration, mineralogy, sequential extractions, Fe(II) release, pH, alkalinity, sulphate removal, glycerol utilisation, and microbial community structure were observed in columns lixiviated with 10 mM glycerol, as compared to organic starved control columns. This is strongly indicative of bioreduction of iron and sulphate in the media in response to biostimulation by microbes. Sequential extractions revealed a redistribution of metals within the various sequential extraction phases in the order Pb>Cu>Zn. Small changes were seen in the Fe distribution. Mineralogy indicated removal of jarosite on the X-ray diffractogram which is consistent with the observed iron and sulphate reduction. The hydrometallurgical extractions performed with HCl, H_2SO_4, citric acid, and EDTA all point to a marked increase in both the leachability of Zn, Cu, and notably Pb and selectivity over Fe. Surprisingly, the highest extraction values were sometimes found for weaker reagent strengths. The largest change was observed in Pb redistribution within various extraction phases, where it moved from least reactive magnetite-targeted and residual phases to more reactive carbonate-targeted and easily reducible oxide phases. This corelates well with the increased leachability of Pb in the period when the column effluent pH remained

low enough to maintain mobility. Furthermore, the chelation extraction was notable in the selectivity of metal removal over Fe – important in extracting value from waste. Post-test analyses indicated the presence of preferential flow paths, indicating that this process needs further optimisation to achieve improved yields. This study can be considered as a foundational work in demonstrating that *in situ* biostimulation of iron-rich jarosite-bearing wastes can lead to iron and sulphate bioreduction and an increase in the subsequent leachability of target metals. This may open-up circular and industrial symbiotic opportunities to biologically manipulate these globally abundant wastes ahead of *in situ* or *ex situ* metal recovery.

Acknowledgements

We would like to thank: Jeff Rowlands and Marco Santonastaso (Cardiff University, School of Engineering) for analytical support, and Natural Resources Wales, Anglesey Mining and the Amlch Industrial Heritage Trust for facilitating access to Parys Mountain. This work was funded by Cardiff University's Engineering and Physical Sciences Research Council (EPSRC) doctoral training partnership EP/M50631X/1 and the UK Natural Environment Research Council (NERC) through grant NE/L013908/1.

Author contributions

Roberts, M. (First Author): Conceptualization, Data curation, Formal analysis, Methodology, Validation, Investigation, Writing - Review & Editing; Srivastava, P. (Corresponding Author): Roles/Writing - original draft; Visualization; Formal Analysis; Webster, G.: Methodology, Validation, and Formal Analysis (for microbial community analysis), Writing - Review & Editing; Weightman, A.: Methodology, Validation, and Formal Analysis (for microbial community analysis), Writing - Review & Editing; Sapsford, D.J: Conceptualization; Methodology; Writing - Original Draft; Visualization; Supervision; Funding acquisition; Project administration

766

767 **REFERENCES:**

768 Bingjie, O., Xiancai, L., Huan, L., Juan, L., Tingting, Z., Xiangyu, Z., Jianjun, L., & Rucheng, W. (2014).
769 Reduction of jarosite by Shewanella oneidensis MR-1 and secondary mineralization. *Geochimica et*
770 *Cosmochimica Acta*, *124*, 54–71. https://doi.org/10.1016/j.gca.2013.09.020

771 Binnemans, K., Pontikes, Y., Jones, P. T., Van, T., & Blanpain, B. (2013). Recovery of Rare Earths From
772 Industrial Waste Residues : a Concise Review. *3rd International Slag Valorisation Symposium*, 191–
773 205.

774 Bonch-Osmolovskaya, E. A. (1994). Bacterial sulfur reduction in hot vents. *FEMS Microbiology Reviews*,
775 *15*(1), 65–77. https://doi.org/10.1111/j.1574-6976.1994.tb00122.x

776 Borra, C. R., Pontikes, Y., Binnemans, K., & van Gerven, T. (2015). Leaching of rare earths from bauxite
777 residue (red mud). *Minerals Engineering*, *76*, 20–27. https://doi.org/10.1016/j.mineng.2015.01.005

778 Bridge, T. A. M., & Johnson, D. B. (1998). Reduction of soluble iron and reductive dissolution of ferric
779 iron- containing minerals by moderately thermophilic iron-oxidizing bacteria. *Applied and*
780 *Environmental Microbiology*, *64*(6), 2181–2186. https://doi.org/10.1128/aem.64.6.2181-2186.1998

781 Brown, G. E., Trainor, T. P., & Chaka, A. M. (2008). Geochemistry of mineral surfaces and factors affecting
782 their chemical reactivity. In *Chemical Bonding at Surfaces and Interfaces*. Elsevier B.V.
783 https://doi.org/10.1016/B978-044452837-7.50008-3

784 Bryan, C. G., Hallberg, K. B., & Johnson, D. B. (2004). Microbial populations in surface spoil at the
785 abandoned Mynydd Parys copper mines. *Mine Water 2004 - Proceedings of the International Mine*
786 *Water Association Symposium*, 107–112. http://hdl.handle.net/10242/37386

787 Caccavo, F., Blakemore, R. P., & Lovley, D. R. (1992). A hydrogen-oxidizing, Fe(III)-reducing
788 microorganism from the Great Bay estuary, New Hampshire. *Applied and Environmental*
789 *Microbiology*, *58*(10), 3211–3216. https://doi.org/10.1128/aem.58.10.3211-3216.1992

790 Castro, L., García-Balboa, C., González, F., Ballester, A., Blázquez, M. L., & Muñoz, J. A. (2013).
791 Effectiveness of anaerobic iron bio-reduction of jarosite and the influence of humic substances.
792 *Hydrometallurgy*, *131–132*, 29–33. https://doi.org/10.1016/j.hydromet.2012.10.005

793 Chapelle, F. H., Bradley, P. M., Thomas, M. A., & McMahon, P. B. (2009). Distinguishing iron-reducing
794 from sulfate-reducing conditions. *Ground Water*, *47*(2), 300–305. https://doi.org/10.1111/j.1745-
795 6584.2008.00536.x

796 Chen, R., Liu, H., Tong, M., Zhao, L., Zhang, P., Liu, D., & Yuan, S. (2018). Impact of Fe(II) oxidation in
797 the presence of iron-reducing bacteria on subsequent Fe(III) bio-reduction. *Science of the Total*
798 *Environment*, *639*, 1007–1014. https://doi.org/10.1016/j.scitotenv.2018.05.241

799 Cho, W. il, & Chung, M. S. (2020). Bacillus spores: a review of their properties and inactivation processing
800 technologies. In *Food Science and Biotechnology* (Vol. 29, Issue 11, pp. 1447–1461).
801 https://doi.org/10.1007/s10068-020-00809-4

Chou, Y. H., Yu, J. H., Liang, Y. M., Wang, P. J., Li, C. W., & Chen, S. S. (2015). Recovery of Cu(II) by chemical reduction using sodium dithionite. *Chemosphere*, *141*, 183–188. https://doi.org/10.1016/j.chemosphere.2015.07.016

Ciriminna, R., Pina, C. della, Rossi, M., & Pagliaro, M. (2014). Understanding the glycerol market. *European Journal of Lipid Science and Technology*, *116*(10), 1432–1439. https://doi.org/10.1002/ejlt.201400229

Connell, W. E., & Patrick, W. H. (1968). Sulfate Reduction in Soil: Effects of Redox Potential and pH. *Science*, *159*(3810), 86–87. https://doi.org/10.1126/science.159.3810.86

Das, A., Mishra, A. K., & Roy, P. (1992). Anaerobic growth on elemental sulfur using dissimilar iron reduction by autotrophic Thiobacillus ferrooxidans. *FEMS Microbiology Letters*, *97*(1–2), 167–172. https://doi.org/10.1016/0378-1097(92)90381-W

Das, G. K., Anand, S., Acharya, S., & Das, R. P. (1997). Characterisation and acid pressure leaching of various nickel-bearing chromite overburden samples. *Hydrometallurgy*, *44*(1–2), 97–111. https://doi.org/10.1016/s0304-386x(96)00034-5

Das, S., Hendry, M. J., & Essilfie-Dughan, J. (2011). Transformation of two-line ferrihydrite to goethite and hematite as a function of pH and temperature. *Environmental Science and Technology*, *45*(1), 268–275. https://doi.org/10.1021/es101903y

Ding, B., Li, Z., & Qin, Y. (2017). Nitrogen loss from anaerobic ammonium oxidation coupled to Iron(III) reduction in a riparian zone. *Environmental Pollution*, *231*, 379–386. https://doi.org/10.1016/j.envpol.2017.08.027

Dong, J., Ding, L., Chi, Z., Lei, J., & Su, Y. (2017). Kinetics of nitrobenzene degradation coupled to indigenous microorganism dissimilatory iron reduction stimulated by emulsified vegetable oil. *Journal of Environmental Sciences (China)*, *54*(Iii), 206–216. https://doi.org/10.1016/j.jes.2016.02.009

dos Santos Afonso, M., & Stumm, W. (1992). Reductive dissolution of iron(III) (hydr)oxides by hydrogen sulfide. *Langmuir*, *8*(6), 1671–1675. https://doi.org/10.1021/la00042a030

Esther, J., Panda, S., Sukla, L. B., Pradhan, N., Sarangi, C. K., & Subbaiah, T. (2015). Enhanced recovery of nickel from chromite overburden (COB) using dissimilatory Fe (III) reducers: A novel Bio-Reduction Acid Leaching (BRAL) approach. *Hydrometallurgy*, *155*, 110–117. https://doi.org/10.1016/j.hydromet.2015.04.019

Esther, J., Pattanaik, A., Pradhan, N., & Sukla, L. B. (2020). Applications of Dissimilatory Iron Reducing Bacteria (DIRB) for recovery of Ni and Co from low-grade lateritic nickel ore. *Materials Today: Proceedings*, *30*, 351–354. https://doi.org/10.1016/j.matpr.2020.02.167

Esther, J., Sukla, L. B., Pradhan, N., & Panda, S. (2015). Fe (III) reduction strategies of dissimilatory iron reducing bacteria. *Korean Journal of Chemical Engineering*, *32*(1), 1–14. https://doi.org/10.1007/s11814-014-0286-x

838 Eusterhues, K., Hädrich, A., Neidhardt, J., Küsel, K., Keller, T. F., Jandt, K. D., & Totsche, K. U. (2014).
839 Reduction of ferrihydrite with adsorbed and coprecipitated organic matter: Microbial reduction by
840 Geobacter bremensis vs. abiotic reduction by Na-dithionite. *Biogeosciences*, *11*(18), 4953–4966.
841 https://doi.org/10.5194/bg-11-4953-2014
842 Falagán, C., Grail, B. M., & Johnson, D. B. (2017). New approaches for extracting and recovering metals
843 from mine tailings. *Minerals Engineering*, *106*, 71–78. https://doi.org/10.1016/j.mineng.2016.10.008
844 Falagán, C., & Johnson, D. B. (2014). Acidibacter ferrireducens gen. nov., sp. nov.: an acidophilic ferric
845 iron-reducing gammaproteobacterium. *Extremophiles*, *18*(6), 1067–1073.
846 https://doi.org/10.1007/s00792-014-0684-3
847 Freyssinet, P. H., Butt, C. R. M., Morris, R. C., & Piantone, P. (2005). Ore-Forming Processes Related to
848 Lateritic Weathering. In J. W. Hedenquist, J. F. H. Thompson, R. J. Goldfarb, & J. P. Richards (Eds.),
849 *One Hundredth Anniversary Volume* (p. 0). Society of Economic Geologists.
850 https://doi.org/10.5382/AV100.21
851 Fuller, S. J., Burke, I. T., McMillan, D. G. G., Ding, W., & Stewart, D. I. (2015). Population changes in a
852 community of alkaliphilic iron-reducing bacteria due to changes in the electron acceptor: Implications
853 for bioremediation at alkaline Cr(VI)-contaminated sites. *Water, Air, and Soil Pollution*, *226*(6).
854 https://doi.org/10.1007/s11270-015-2437-z
855 Gramp, J. P., Wang, H., Bigham, J. M., Sandy Jones, F., & Tuovinen, O. H. (2009). Biogenic synthesis and
856 reduction of Fe(III)-hydroxysulfates. *Geomicrobiology Journal*, *26*(4), 275–280.
857 https://doi.org/10.1080/01490450902892597
858 Greene, A. C., & Sheehy, A. J. (1997). Defem'bacter themzophilus. *Strain*, *47*(2), 505–509.
859 Gupta, R. S., & Gao, B. (2009). Phylogenomic analyses of clostridia and identification of novel protein
860 signatures that are specific to the genus Clostridium sensu stricto (cluster I). *International Journal of*
861 *Systematic and Evolutionary Microbiology*, *59*(2), 285–294. https://doi.org/10.1099/ijs.0.001792-0
862 Hallberg, K. B., Grail, B. M., Plessis, C. A. D., & Johnson, D. B. (2011). Reductive dissolution of ferric
863 iron minerals: A new approach for bio-processing nickel laterites. *Minerals Engineering*, *24*(7), 620–
864 624. https://doi.org/10.1016/j.mineng.2010.09.005
865 Han, H., Sun, W., Hu, Y., Jia, B., & Tang, H. (2014). Anglesite and silver recovery from jarosite residues
866 through roasting and sulfidization-flotation in zinc hydrometallurgy. *Journal of Hazardous Materials*,
867 *278*, 49–54. https://doi.org/10.1016/j.jhazmat.2014.05.091
868 Hansel, C. M., Lentini, C. J., Tang, Y., Johnston, D. T., Wankel, S. D., & Jardine, P. M. (2015). Dominance
869 of sulfur-fueled iron oxide reduction in low-sulfate freshwater sediments. *ISME Journal*, *9*(11), 2400–
870 2412. https://doi.org/10.1038/ismej.2015.50
871 Hedin, R. (2003). Recovery of marketable iron oxide from mine drainage in the USA. *Land Contamination*
872 *\& Reclamation*, *11*, 93–97.

873 Hernández, C. M. F., Banza, A. N., & Gock, E. (2007). Recovery of metals from Cuban nickel tailings by
874 leaching with organic acids followed by precipitation and magnetic separation. *Journal of Hazardous*
875 *Materials*, *139*(1), 25–30. https://doi.org/10.1016/j.jhazmat.2006.03.074
876 *International - U.S. Energy Information Administration (EIA)*. (n.d.). Retrieved 12 September 2022, from
877 https://www.eia.gov/international/data/world/biofuels/biofuels-
878 production?pd=79&p=000003g&u=1&f=A&v=mapbubble&a=-
879 &i=none&vo=value&t=C&g=00000000000000000000000000000000000000000000001&l=249
880 -ruvvvvvfvtvnvv1vrvvvvfvvvvvvfvvvou20evvvvvvvvvvnvvvs0008&s=315
881 IVARSON, K. C., HALLBERG, R. O., & WADSTEN, T. (1976). the Pyritization of Basic Ferric Sulfates
882 in Acid Sulfate Soils: a Microbiological Interpretation. *Canadian Journal of Soil Science*, *56*(4), 393–
883 406. https://doi.org/10.4141/cjss76-048
884 Jenkins, D. A., Johnson, D. B., & Freeman, C. (2000). Mynydd Parys Cu-Pb-Zn Mines: mineralogy,
885 microbiology and acid mine drainage. In J. D. Cotter-Howells, L. S. Campbell, E. Valsami-Jones, &
886 M. Batchelder (Eds.), *Environmental Mineralogy: Microbial Interactions, Anthropogenic Influences,*
887 *Contaminated Land and Waste Management* (Vol. 9, p. 0). Mineralogical Society of Great Britain and
888 Ireland. https://doi.org/10.1180/MSS.9.9
889 Johansson, N., Krook, J., Eklund, M., & Berglund, B. (2013). An integrated review of concepts and
890 initiatives for mining the technosphere: Towards a new taxonomy. *Journal of Cleaner Production*, *55*,
891 35–44. https://doi.org/10.1016/j.jclepro.2012.04.007
892 Jones, E. J. P., Nadeau, T. L., Voytek, M. A., & Landa, E. R. (2006). Role of microbial iron reduction in
893 the dissolution of iron hydroxysulfate minerals. *Journal of Geophysical Research: Biogeosciences*,
894 *111*(1), 1–8. https://doi.org/10.1029/2005JG000089
895 Ju, S., Zhang, Y., Zhang, Y., Xue, P., & Wang, Y. (2011). Clean hydrometallurgical route to recover zinc,
896 silver, lead, copper, cadmium and iron from hazardous jarosite residues produced during zinc
897 hydrometallurgy. *Journal of Hazardous Materials*, *192*(2), 554–558.
898 https://doi.org/10.1016/j.jhazmat.2011.05.049
899 Lee, J. chun, & Pandey, B. D. (2012). Bio-processing of solid wastes and secondary resources for metal
900 extraction - A review. *Waste Management*, *32*(1), 3–18.
901 https://doi.org/10.1016/j.wasman.2011.08.010
902 Legodi, M. A., & de Waal, D. (2007). The preparation of magnetite, goethite, hematite and maghemite of
903 pigment quality from mill scale iron waste. *Dyes and Pigments*, *74*(1), 161–168.
904 https://doi.org/10.1016/j.dyepig.2006.01.038
905 Li, X. M., Zhou, S. G., Li, F. B., Wu, C. Y., Zhuang, L., Xu, W., & Liu, L. (2009). Fe(III) oxide reduction
906 and carbon tetrachloride dechlorination by a newly isolated Klebsiella pneumoniae strain L17. *Journal*
907 *of Applied Microbiology*, *106*(1), 130–139. https://doi.org/10.1111/j.1365-2672.2008.03985.x

908 Li, Y. L., Vali, H., Yang, J., Phelps, T. J., & Zhang, C. L. (2006). Reduction of iron oxides enhanced by a
909 sulfate-reducing bacterium and biogenic H2S. *Geomicrobiology Journal*, *23*(2), 103–117.
910 https://doi.org/10.1080/01490450500533965
911 Liu, C., Ju, S. H., Zhang, L. B., Srinivasakannan, C., Peng, J. H., Le, T. Q. X., & Guo, Z. Y. (2017).
912 Recovery of valuable metals from jarosite by sulphuric acid roasting using microwave and water
913 leaching. *Canadian Metallurgical Quarterly*, *56*(1), 1–9.
914 https://doi.org/10.1080/00084433.2016.1242972
915 Liu, Y., & Naidu, R. (2014). Hidden values in bauxite residue (red mud): Recovery of metals. *Waste*
916 *Management*, *34*(12), 2662–2673. https://doi.org/10.1016/j.wasman.2014.09.003
917 Lonergan, D. J., Jenter, H. L., Coates, J. D., Phillips, E. J. P., Schmidt, T. M., & Lovley, D. R. (1996).
918 Phylogenetic analysis of dissimilatory Fe(III)-reducing bacteria. *Journal of Bacteriology*, *178*(8),
919 2402–2408. https://doi.org/10.1128/jb.178.8.2402-2408.1996
920 Lovley, D. (1993). Dissimilatory Metal Reduction. *Annual Review of Microbiology*, *47*(1), 263–290.
921 https://doi.org/10.1146/annurev.micro.47.1.263
922 Lovley, D. (2013). *Dissimilatory Fe(III)- and Mn(IV)-Reducing Prokaryotes BT - The Prokaryotes:*
923 *Prokaryotic Physiology and Biochemistry* (E. Rosenberg, E. F. DeLong, S. Lory, E. Stackebrandt, &
924 F. Thompson, Eds.; pp. 287–308). Springer Berlin Heidelberg. https://doi.org/10.1007/978-3-642-
925 30141-4_69
926 Lovley, D. R., & Phillips, E. J. P. (1987). Competitive Mechanisms for Inhibition of Sulfate Reduction and
927 Methane Production in the Zone of Ferric Iron Reduction in Sediments. *Applied and Environmental*
928 *Microbiology*, *53*(11), 2636–2641. https://doi.org/10.1128/aem.53.11.2636-2641.1987
929 Markova, N., Slavchev, G., Michailova, L., & Jourdanova, M. (2010). Survival of Escherichia coli under
930 lethal heat stress by L-form conversion. *International Journal of Biological Sciences*, *6*(4), 303–315.
931 https://doi.org/10.7150/ijbs.6.303
932 Marsh, E., & Anderson, E. (2011). Ni-Co laterites - a deposit model. *US Geological Survey Open-File*
933 *Report*, *1259*, 1–12. http://pubs.usgs.gov/of/2011/1259/OF11-1259.pdf
934 Mudd, G. M., & Boger, D. v. (2013). The ever growing case for paste and thickened tailings - Towards
935 more sustainable mine waste management. *AusIMM Bulletin*, *2*, 56–59.
936 Ňancucheo, I., Grail, B. M., Hilario, F., du Plessis, C., & Johnson, D. B. (2014). Extraction of copper from
937 an oxidized (lateritic) ore using bacterially catalysed reductive dissolution. *Applied Microbiology and*
938 *Biotechnology*, *98*(14), 6297–6305. https://doi.org/10.1007/s00253-014-5687-6
939 ñancucheo, I., Oliveira, R., Dall'Agnol, H., Barrie Johnson, D., Grail, B., Holanda, R., Nunes, G. L.,
940 Cuadros-Orellana, S., & Oliveira, G. (2016). Draft genome sequence of a novel acidophilic iron-
941 oxidizing Firmicutes species, 'Acidibacillus ferrooxidans' (SLC66T). *Genome Announcements*, *4*(3),
942 53–54. https://doi.org/10.1128/genomeA.00383-16

943 Natarajan, K. (2015). Biomineralisation and Microbially Induced Beneficiation. In *Microbiology for*
944 *Minerals, Metals, Materials and the Environment* (pp. 1–34). CRC Press.
945 https://doi.org/10.1201/b18124-2
946 Novais, R. M., Seabra, M. P., Amaral, J. S., & Pullar, R. C. (2016). Hidden value in low-cost inorganic
947 pigments as potentially valuable magnetic materials. *Ceramics International*, *42*(8), 9605–9612.
948 https://doi.org/10.1016/j.ceramint.2016.03.045
949 Ojumu, T. v., Hansford, G. S., & Petersen, J. (2009). The kinetics of ferrous-iron oxidation by
950 Leptospirillum ferriphilum in continuous culture: The effect of temperature. *Biochemical Engineering*
951 *Journal*, *46*(2), 161–168. https://doi.org/10.1016/j.bej.2009.05.001
952 Osorio, H., Mangold, S., Denis, Y., Ñancucheo, I., Esparza, M., Johnson, D. B., Bonnefoy, V., Dopson,
953 M., & Holmesa, D. S. (2013). Anaerobic sulfur metabolism coupled to dissimilatory iron reduction in
954 the extremophile Acidithiobacillus ferrooxidans. *Applied and Environmental Microbiology*, *79*(7),
955 2172–2181. https://doi.org/10.1128/AEM.03057-12
956 O'Sullivan, L. A., Roussel, E. G., Weightman, A. J., Webster, G., Hubert, C. R. J., Bell, E., Head, I., Sass,
957 H., & John Parkes, R. (2015). Survival of Desulfotomaculum spores from estuarine sediments after
958 serial autoclaving and high-temperature exposure. *ISME Journal*, *9*, 922–933.
959 https://doi.org/10.1038/ismej.2014.190
960 Papassiopi, N., Vaxevanidou, K., & Paspaliaris, I. (2010). Effectiveness of iron reducing bacteria for the
961 removal of iron from bauxite ores. *Minerals Engineering*, *23*(1), 25–31.
962 https://doi.org/10.1016/j.mineng.2009.09.005
963 Pelino, M., Cantalini, C., & Rincon, J. M. (1997). Preparation and properties of glass-ceramic materials
964 obtained by recycling goethite industrial waste. *Journal of Materials Science*, *32*(17), 4655–4660.
965 https://doi.org/10.1023/A:1018602224392
966 Pollock, J., Weber, K. A., Lack, J., Achenbach, L. A., Mormile, M. R., & Coates, J. D. (2007). Alkaline
967 iron(III) reduction by a novel alkaliphilic, halotolerant, Bacillus sp. isolated from salt flat sediments
968 of Soap Lake. *Applied Microbiology and Biotechnology*, *77*(4), 927–934.
969 https://doi.org/10.1007/s00253-007-1220-5
970 Poulton, S. W., & Canfield, D. E. (2005). Development of a sequential extraction procedure for iron:
971 Implications for iron partitioning in continentally derived particulates. *Chemical Geology*, *214*(3–4),
972 209–221. https://doi.org/10.1016/j.chemgeo.2004.09.003
973 Power, G., Gräfe, M., & Klauber, C. (2011). Bauxite residue issues: I. Current management, disposal and
974 storage practices. *Hydrometallurgy*, *108*(1–2), 33–45. https://doi.org/10.1016/j.hydromet.2011.02.006
975 Rickard, D., & Morse, J. W. (2005). Acid volatile sulfide (AVS). In *Marine Chemistry* (Vol. 97, Issues 3–
976 4). https://doi.org/10.1016/j.marchem.2005.08.004
977 Riedinger, N., Brunner, B., Krastel, S., Arnold, G. L., Wehrmann, L. M., Formolo, M. J., Beck, A., Bates,
978 S. M., Henkel, S., Kasten, S., & Lyons, T. W. (2017). Sulfur cycling in an iron oxide-dominated,

dynamic marine depositional system: The argentine continental margin. *Frontiers in Earth Science*, *5*(May). https://doi.org/10.3389/feart.2017.00033

Roberts, M., Weightman, A., & Sapsford, D. J. (2020). Chapter 8 Potential Application of Direct and Indirect Iron Bioreduction in Resource Recovery from Iron Oxide-bearing Wastes. In *Resource Recovery from Wastes: Towards a Circular Economy* (pp. 192–212). The Royal Society of Chemistry. https://doi.org/10.1039/9781788016353-00192

Rochelle, P. A., Weightman, A. J., & Fry, J. C. (1992). DNase I treatment of Taq DNA polymerase for complete PCR decontamination. *BioTechniques*, *13*(4), 520.

Royer-Lavallée, A., Neculita, C. M., & Coudert, L. (2020). Removal and potential recovery of rare earth elements from mine water. *Journal of Industrial and Engineering Chemistry*, *89*, 47–57. https://doi.org/10.1016/j.jiec.2020.06.010

Ryan, M. J., Kney, A. D., & Carley, T. L. (2017). A study of selective precipitation techniques used to recover refined iron oxide pigments for the production of paint from a synthetic acid mine drainage solution. *Applied Geochemistry*, *79*, 27–35. https://doi.org/10.1016/j.apgeochem.2017.01.019

Sapsford, D., Santonastaso, M., Thorn, P., & Kershaw, S. (2015). Conversion of coal mine drainage ochre to water treatment reagent: Production, characterisation and application for P and Zn removal. *Journal of Environmental Management*, *160*, 7–15. https://doi.org/10.1016/j.jenvman.2015.06.004

Shiers, D. W., Collinson, D. M., & Watling, H. R. (2016). Life in heaps: a review of microbial responses to variable acidity in sulfide mineral bioleaching heaps for metal extraction. *Research in Microbiology*, *167*(7), 576–586. https://doi.org/10.1016/j.resmic.2016.05.007

Shuai, W., & Jaffé, P. R. (2019). Anaerobic ammonium oxidation coupled to iron reduction in constructed wetland mesocosms. *Science of the Total Environment*, *648*, 984–992. https://doi.org/10.1016/j.scitotenv.2018.08.189

Sillitoe, R. H., & Perelló, J. (2005). Andean Copper Province: Tectonomagmatic Settings, Deposit Types, Metallogeny, Exploration, and Discovery. In J. W. Hedenquist, J. F. H. Thompson, R. J. Goldfarb, & J. P. Richards (Eds.), *One Hundredth Anniversary Volume* (p. 0). Society of Economic Geologists. https://doi.org/10.5382/AV100.26

Silva, A. M. N., Kong, X., Parkin, M. C., Cammack, R., & Hider, R. C. (2009). Iron(iii) citrate speciation in aqueous solution. *Dalton Transactions*, *40*, 8616–8625. https://doi.org/10.1039/b910970f

Sintorini, M. M., Widyatmoko, H., Sinaga, E., & Aliyah, N. (2021). Effect of pH on metal mobility in the soil. *IOP Conference Series: Earth and Environmental Science*, *737*(1), 6–12. https://doi.org/10.1088/1755-1315/737/1/012071

Smeaton, C. M., Walshe, G. E., Smith, A. M. L., Hudson-Edwards, K. A., Dubbin, W. E., Wright, K., Beale, A. M., Fryer, B. J., & Weisener, C. G. (2012). Simultaneous release of Fe and As during the reductive dissolution of Pb-As jarosite by Shewanella putrefaciens CN32. *Environmental Science and Technology*, *46*(23), 12823–12831. https://doi.org/10.1021/es3021809

1015 Smith, S. L., Grail, B. M., & Johnson, D. B. (2017). Reductive bioprocessing of cobalt-bearing limonitic
1016 laterites. *Minerals Engineering*, *106*, 86–90. https://doi.org/10.1016/j.mineng.2016.09.009
1017 Spring, S., & Rosenzweig, F. (2006). *The Genera Desulfitobacterium and Desulfosporosinus: Taxonomy*
1018 *BT - The Prokaryotes: Volume 4: Bacteria: Firmicutes, Cyanobacteria* (M. Dworkin, S. Falkow, E.
1019 Rosenberg, K.-H. Schleifer, & E. Stackebrandt, Eds.; pp. 771–786). Springer US.
1020 https://doi.org/10.1007/0-387-30744-3_24
1021 Srivastava, P., Al-Obaidi, S. A., Webster, G., Weightman, A. J., & Sapsford, D. J. (2022). Towards passive
1022 bioremediation of dye-bearing effluents using hydrous ferric oxide wastes: Mechanisms, products and
1023 microbiology. *Journal of Environmental Management*, *317*(May), 115332.
1024 https://doi.org/10.1016/j.jenvman.2022.115332
1025 Stern, N., Mejia, J., He, S., Yang, Y., Ginder-Vogel, M., & Roden, E. E. (2018). Dual Role of Humic
1026 Substances As Electron Donor and Shuttle for Dissimilatory Iron Reduction. *Environmental Science*
1027 *and Technology*, *52*(10), 5691–5699. https://doi.org/10.1021/acs.est.7b06574
1028 Straub, K. L., Hanzlik, M., & Buchholz-Cleven, B. E. E. (1998). The use of biologically produced
1029 ferrihydrite for the isolation of novel iron-reducing bacteria. *Systematic and Applied Microbiology*,
1030 *21*(3), 442–449. https://doi.org/10.1016/S0723-2020(98)80054-4
1031 Sun, B., Zhao, F. J., Lombi, E., & McGrath, S. P. (2001). Leaching of heavy metals from contaminated
1032 soils using EDTA. *Environmental Pollution*, *113*(2), 111–120. https://doi.org/10.1016/S0269-
1033 7491(00)00176-7
1034 Tamaura, Y., Katsura, T., Rojarayanont, S., Yoshida, T., & Abe, H. (1991). Ferrite Process; Heavy Metal
1035 Ions Treatment System. *Water Science and Technology*, *23*(10–12), 1893–1900.
1036 https://doi.org/10.2166/wst.1991.0645
1037 Thornton, I., Rautiu, R., & Brush, S. (2001). Lead: the facts. *IC Consultants Ltd, London, UK*.
1038 Vargas, M., Kashefi, K., Blunt-harris, E. L., & Lovley, D. R. (1998). Fe (III) reduction on early Earth.
1039 *Nature*, *395*(September), 65–67.
1040 Vaxevanidou, K., Christou, C., Kremmydas, G. F., Georgakopoulos, D. G., & Papassiopi, N. (2015). Role
1041 of indigenous arsenate and IRON(III) respiring microorganisms in controlling the mobilization of
1042 arsenic in a contaminated soil sample. *Bulletin of Environmental Contamination and Toxicology*,
1043 *94*(3), 282–288. https://doi.org/10.1007/s00128-015-1458-z
1044 Vaziri Hassas, B., Rezaee, M., & Pisupati, S. v. (2020). Precipitation of rare earth elements from acid mine
1045 drainage by CO2 mineralization process. *Chemical Engineering Journal*, *399*(March), 125716.
1046 https://doi.org/10.1016/j.cej.2020.125716
1047 Villemur, R., Lanthier, M., Beaudet, R., & Lépine, F. (2006). The Desulfitobacterium genus. *FEMS*
1048 *Microbiology Reviews*, *30*(5), 706–733. https://doi.org/10.1111/j.1574-6976.2006.00029.x

Wang, W., Pranolo, Y., & Cheng, C. Y. (2013). Recovery of scandium from synthetic red mud leach solutions by solvent extraction with D2EHPA. *Separation and Purification Technology*, *108*, 96–102. https://doi.org/10.1016/j.seppur.2013.02.001

Wang, W., Zhenghe, X. U., & Finch, J. (1996). Fundamental study of an ambient temperature ferrite process in the treatment of acid mine drainage. *Environmental Science and Technology*, *30*(8), 2604–2608. https://doi.org/10.1021/es960006h

Weber, K. A., Urrutia, M. M., Churchill, P. F., Kukkadapu, R. K., & Roden, E. E. (2006). Anaerobic redox cycling of iron by freshwater sediment microorganisms. *Environmental Microbiology*, *8*(1), 100–113. https://doi.org/10.1111/j.1462-2920.2005.00873.x

Webster, G., Newberry, C. J., Fry, J. C., & Weightman, A. J. (2003). Assessment of bacterial community structure in the deep sub-seafloor biosphere by 16S rDNA-based techniques: A cautionary tale. *Journal of Microbiological Methods*, *55*(1), 155–164. https://doi.org/10.1016/S0167-7012(03)00140-4

Xu, P., Zeng, G. M., Huang, D. L., Feng, C. L., Hu, S., Zhao, M. H., Lai, C., Wei, Z., Huang, C., Xie, G. X., & Liu, Z. F. (2012). Use of iron oxide nanomaterials in wastewater treatment: A review. *Science of the Total Environment*, *424*, 1–10. https://doi.org/10.1016/j.scitotenv.2012.02.023

Xu, Y., He, Y., Feng, X., Liang, L., Xu, J., Brookes, P. C., & Wu, J. (2014). Enhanced abiotic and biotic contributions to dechlorination of pentachlorophenol during Fe(III) reduction by an iron-reducing bacterium Clostridium beijerinckii Z. *Science of the Total Environment*, *473–474*, 215–223. https://doi.org/10.1016/j.scitotenv.2013.12.022

Yang, F., Hanna, M. A., & Sun, R. (2012). Yang et al. 2012 value added use crude glycerol. *Biotechnology for Biofuels*, *5*(1), 1–10.

Yang, J., Zhang, S. G., Pan, D. A., Liu, B., Wu, C. L., & Volinsky, A. A. (2016). Treatment method of hazardous pickling sludge by reusing as glass–ceramics nucleation agent. *Rare Metals*, *35*(3), 269–274. https://doi.org/10.1007/s12598-015-0673-4

Zachara, J. M., Fredrickson, J. K., Smith, S. C., & Gassman, P. L. (2001). Solubilization of Fe(III) oxide-bound trace metals by a dissimilatory Fe(III) reducing bacterium. *Geochimica et Cosmochimica Acta*, *65*(1), 75–93. https://doi.org/10.1016/S0016-7037(00)00500-7

Zavarzina, D. G., Sokolova, T. G., Tourova, T. P., Chernyh, N. A., Kostrikina, N. A., & Bonch-Osmolovskaya, E. A. (2007). Thermincola ferriacetica sp. nov., a new anaerobic, thermophilic, facultatively chemolithoautotrophic bacterium capable of dissimilatory Fe(III) reduction. *Extremophiles*, *11*(1), 1–7. https://doi.org/10.1007/s00792-006-0004-7

Zhang, J., Wang, Y., Muldoon, V. L., & Deng, S. (2022). Crude glycerol and glycerol as fuels and fuel additives in combustion applications. *Renewable and Sustainable Energy Reviews*, *159*(February), 112206. https://doi.org/10.1016/j.rser.2022.112206

Zhong, L. S., Hu, J. S., Liang, H. P., Cao, A. M., Song, W. G., & Wan, L. J. (2006). Self-assembled 3D flowerlike iron oxide nanostructures and their application in water treatment. *Advanced Materials*, *18*(18), 2426–2431. https://doi.org/10.1002/adma.200600504

Ziegler, S., Waidner, B., Itoh, T., Schumann, P., Spring, S., & Gescher, J. (2013). Metallibacterium scheffleri gen. nov., sp. nov., an alkalinizing gammaproteobacterium isolated from an acidic biofilm. *International Journal of Systematic and Evolutionary Microbiology*, *63*(PART4), 1499–1504. https://doi.org/10.1099/ijs.0.042986-0

Figures with captions

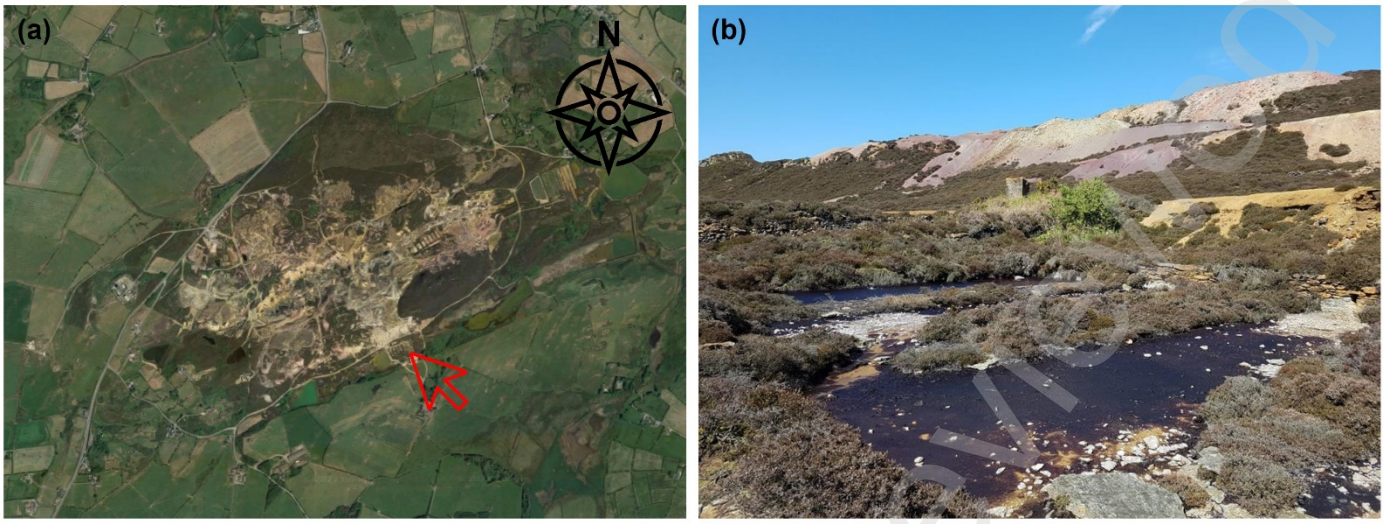

Figure 1 (a) Aerial view of Parys Mountain mine, N. Wales. The red arrow indicates the sampling location (53°23'13 N, 4°20'37 W). Image copyright Google Earth™ 2022 Google, Imagery; (b) Picture of the sampling location on Parys Mt. Note the algal mats on the waste surface.

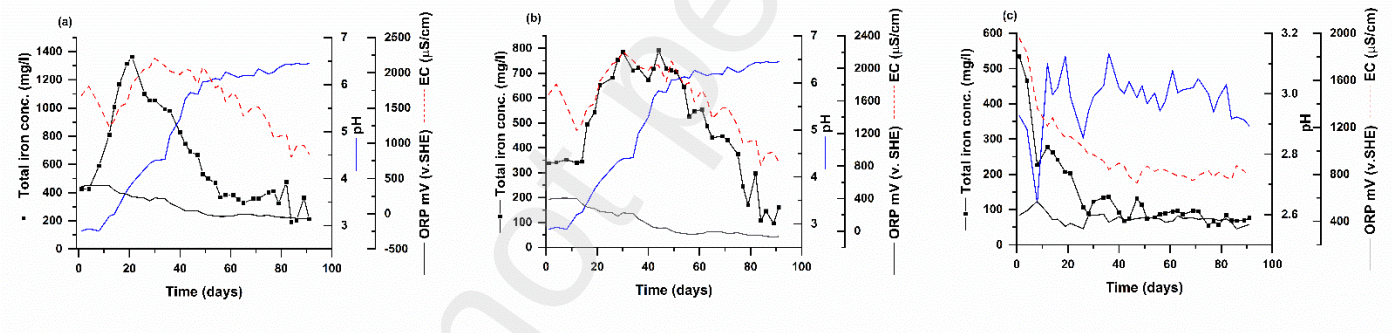

Figure 2 Changes in the physicochemical properties like pH, conductivity, and the oxidation-reduction potential in comparison to the total iron of the column effluents from (a) organic starved, (b) live, and (c) autoclaved column. Please note the difference in the axes.

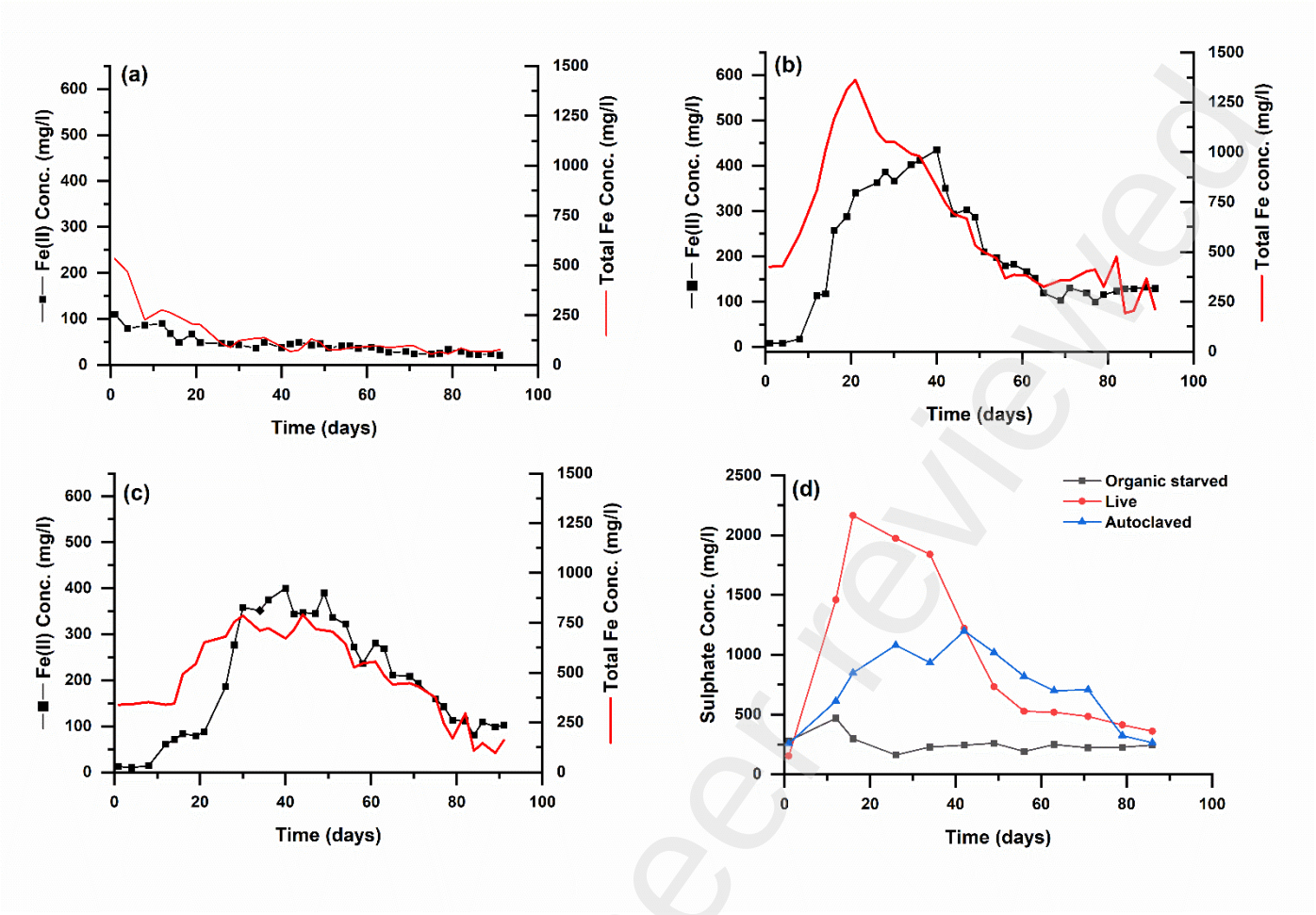

Figure 3 Fe(II) released over time in comparison to the total iron present in the effluents from (a) organic starved, (b) live, and (c) autoclaved columns; (d) Changes in the sulphate concentration in the column effluents, with live columns exhibiting the highest release at around day 20.

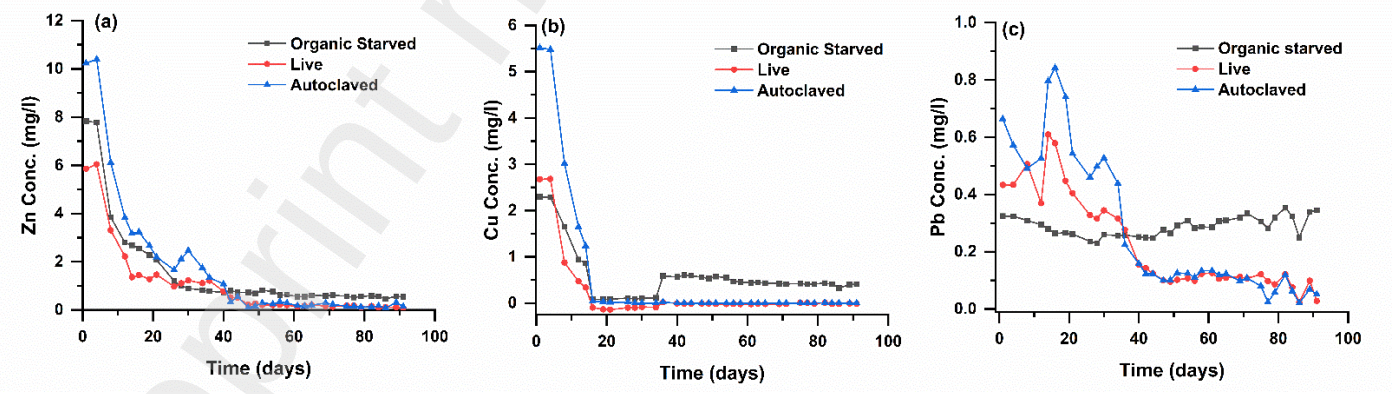

Figure 4 Effect of biostimulation on the trend of release of metals (a) Zn, (b) Cu, and (c) Pb in column effluents. Please note the different in the axes.

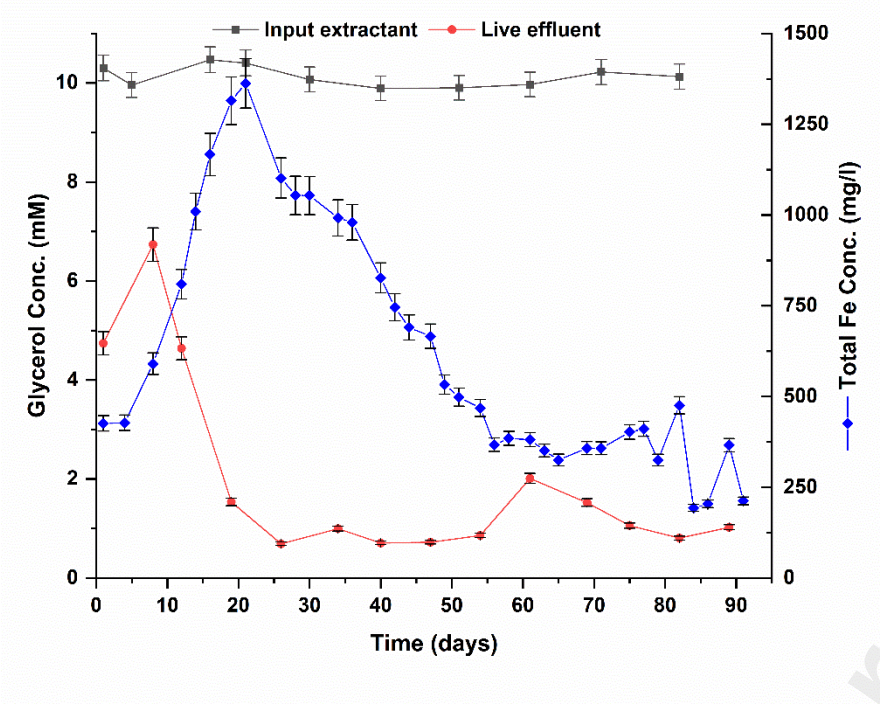

Figure 5 Decrease in glycerol concentration in the effluent from live columns when compared to input extractant and its relationship with the changes in the total iron concentration.

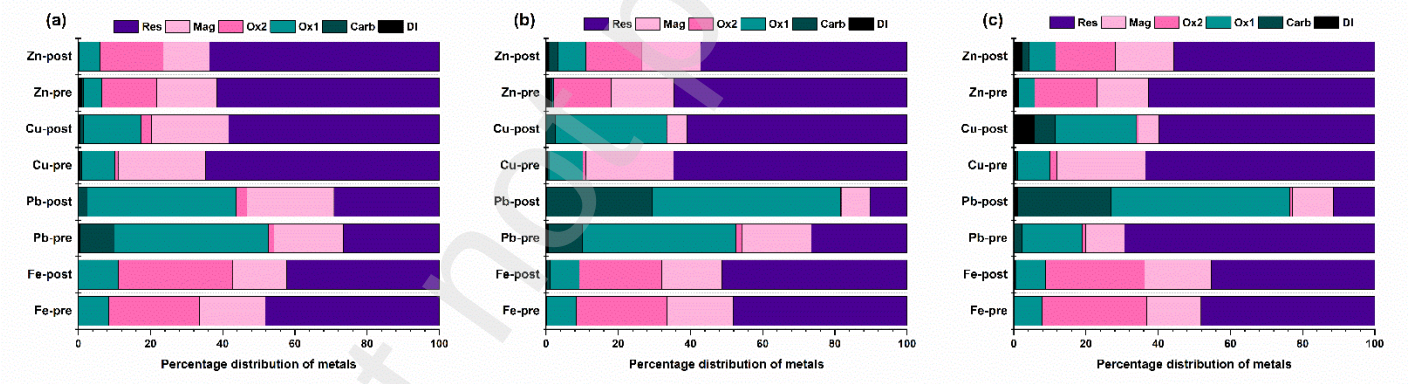

Figure 6 Comparison of sequential extraction of Fe, Zn, Cu, and Pb from pre- and post-experiment wastes from (a) organic starved, (b) lives, and (c) autoclaved columns post biostimulation. (Res- residual phase; Mag- magnetite targeted phase; Ox2- reducible oxide phase; Ox1- readily reducible oxide phase; Carb- carbonate associate phase; DI- water soluble phase).

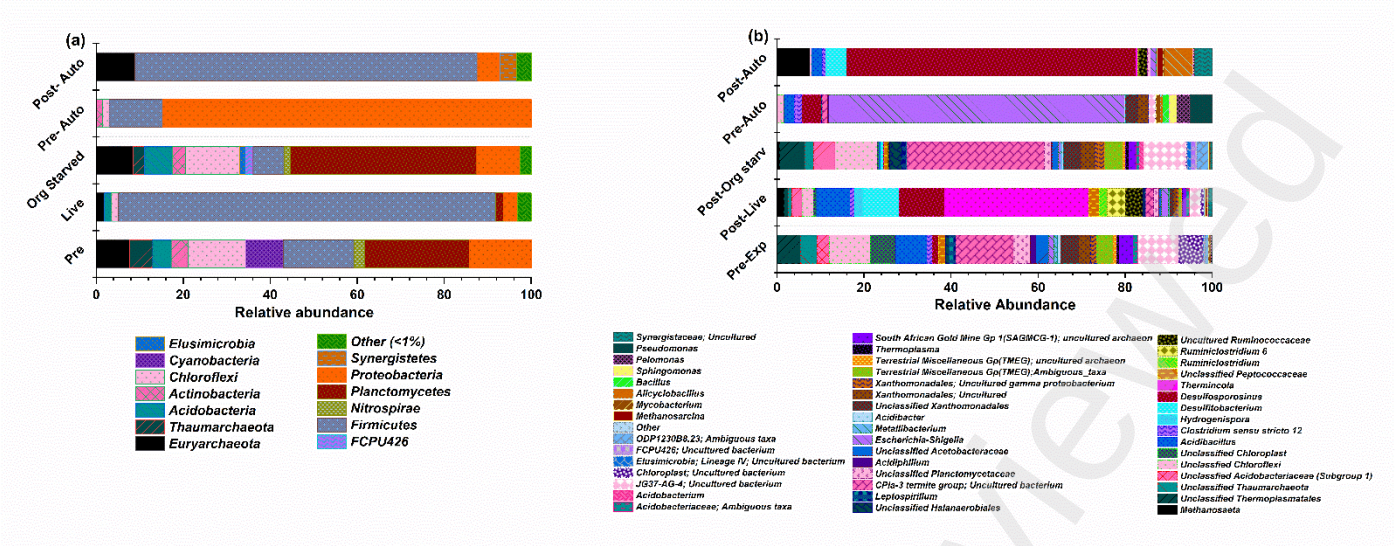

Figure 7 Changes in microbial community structure exhibited by the Parys Mt waste pre- and post-experiment, in organic starved, live, and autoclaved columns when fed with BTEX containing influent at (a) phylum level and (b) genus level. (Auto- autoclaved)

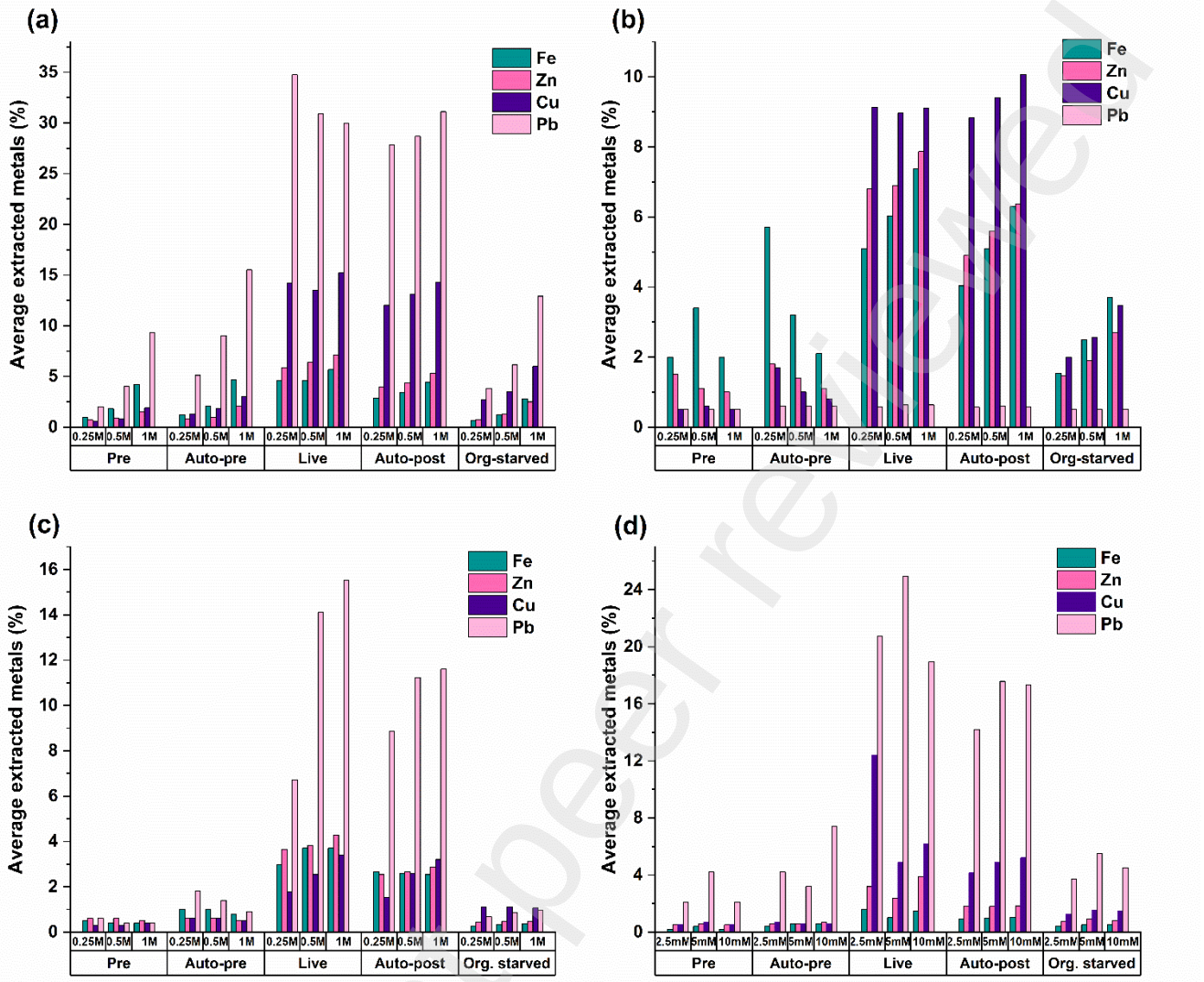

Figure 8 Leachability of metals from Parys Mt. (Pre), organic starved (Org. Starved), live, autoclaved Parys Mt (Auto-Pre), and autoclaved wastes (Auto-Post) when (a) HCl, (b) H_2SO_4, (c) citric acid ($C_6H_8O_7$), and EDTA were used as lixiviants.